



7-Azaindole-1-carboxamides as a new class of PARP-1 inhibitors

Raffaella Cincinelli^{a,†}, Loana Musso^{a,†}, Lucio Merlini^a, Giuseppe Giannini^b, Loredana Vesci^b, Ferdinando M. Milazzo^b, Nives Carenini^c, Paola Perego^c, Sergio Penco^b, Roberto Artali^d, Franco Zunino^c, Claudio Pisano^b, Sabrina Dallavalle^{a,*}

^a Department of Food, Environmental and Nutritional Sciences, Division of Chemistry and Molecular Biology, Università di Milano, via Celoria 2, 20133 Milano, Italy

^b R&D Sigma-Tau Industrie Farmaceutiche Riunite S.p.A., via Pontina Km 30, 400, I-00040 Pomezia (RM), Italy

^c Molecular Pharmacology Unit, Dept. Experimental Oncology and Molecular Medicine, Fondazione IRCCS Istituto Nazionale Tumori, via Amadeo 42, I-20133 Milan, Italy

^d Scientia Advice, di Roberto Artali, 20832 Desio (MB), Italy

ARTICLE INFO

Article history:

Received 25 October 2013

Revised 12 December 2013

Accepted 16 December 2013

Available online 22 December 2013

Keywords:

PARP inhibitors

Synthesis

Molecular modelling

7-Azaindoles

Antitumor

ABSTRACT

7-Azaindole-1-carboxamides were designed as a new class of PARP-1 inhibitors. The compounds displayed a variable pattern of target inhibition profile that, in part, paralleled the antiproliferative activity in cell lines characterized by homologous recombination defects. A selected compound (**11**; ST7710AA1) showed significant in vitro target inhibition and capability to substantially bypass the multidrug resistance mediated by Pgp. In antitumor activity studies against the MX1 human breast carcinoma growth in nude mice, the compound exhibited an effect similar to that of Olaparib in terms of tumor volume inhibition when used at a lower dose than the reference compound. Treatment was well tolerated, as no deaths or significant weight losses were observed among the treated animals.

© 2013 Elsevier Ltd. All rights reserved.

1. Introduction

Members of the Poly(ADP-ribose) polymerase (PARP) proteins family are promising therapeutic targets which are involved in maintaining DNA integrity and in regulation of programmed cell death.^{1,2} So far 18 members have been described, PARP-1 and PARP-2 being the best characterized ones. PARP-1, which is selectively activated by DNA damage, catalyzes the transfer of ADP-ribose units to a variety of nuclear proteins (histones, transcription factors and PARP itself) using nicotinamide adenine dinucleotide (NAD⁺) as a substrate, thereby leading to the formation of long and branched poly(ADP-ribose)(PAR) chains.³ This is a key process for the repair of DNA damage through the base excision repair (BER) pathway.³

Given the biological role of the enzyme, the blockade of PARP-1 activity has the potential to prevent DNA damage repair leading consequently to cell death. Since the efficacy of many anticancer drugs implicating DNA damage is undermined by the emergence of resistance, often due to enhanced DNA repair, PARP-1 inhibitors have also potential therapeutic applications as chemo-sensitizers. PARP inhibitors have been reported to sensitize cancer cells to drug

and radiation treatment,^{2,4} and clinical trials of combinations with DNA-damaging agents are in progress.^{4b}

Moreover, cells carrying mutations in BRCA1/2 tumor suppressor genes are sensitive to PARP inhibitors *per se* owing to their defect in homologous recombination.^{5,6} Thus, PARP inhibitors are promising agents as monotherapy in patients with mutated BRCA genes.⁷ In this context, PARP inhibition results in synthetic lethality of cells characterized by homologous recombination defects.⁸

In addition to cancer, PARP-1 has been shown to be involved in other disease conditions including inflammation,⁹ neuronal death and ischemia.¹⁰

In the last three decades, a large number of PARP-1 inhibitors have been reported,^{11,12} including Veliparib, 3AB, Olaparib, Rucaparib and Niraparib (Fig 1). Some of them are in advanced clinical trials as single agents or in combination with DNA-damaging drugs.^{4b,13,14}

Most of the PARP inhibitors developed to date are structural analogues of nicotinamide, and are thought to compete with NAD itself at the level of the catalytic domain.

The human PARP proteins share only between 18% and 45% sequence homology in their catalytic domains, but crystal data indicate that their structure is conserved and the mode of NAD⁺ cofactor binding is rather similar. Indeed, X-ray crystal structures^{11,12} and molecular modelling studies^{15–18} indicated that the amide of nicotinamide makes three key hydrogen bonds with the hydroxyl group of a serine residue and the amide backbone of a

* Corresponding author. Tel.: +39 02 50316818; fax: +39 02 50316801.

E-mail address: sabrina.dallavalle@unimi.it (S. Dallavalle).

† These authors contributed equally to the study.

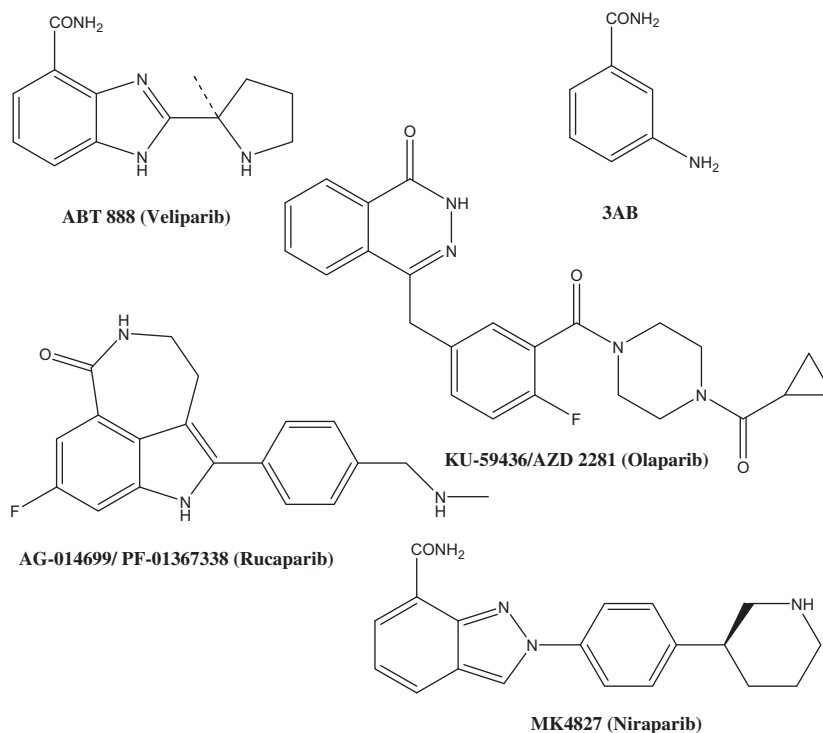


Figure 1. Structure of PARP inhibitors.

glycine residue, and that there is a stacking interaction with a conserved tyrosine residue. All the available structures of PARP inhibitor complexes show compound bound to the pocket which retains this moiety after NAD^+ cleavage. One of the simplest compounds, 3-AB (Fig. 1), resembles nicotinamide and has been cocrystallized with several PARP proteins. Extension of the compounds into the donor site and toward the acceptor loops was used to improve affinity and isoform selectivity. The success of this concept is illustrated considering the structure of the complex with ABT-888.^{19,20}

The synthesis of conformationally constrained cyclic derivatives of benzamide has demonstrated the crucial role of an anti-disposition of the amide bond. Thus, attempts to improve the affinity of PARP inhibitors to the binding site have been made by locking the carboxamide group, which is usually free to rotate, into the desired anti-conformation (Fig. 2).¹¹

In the present work, new 6-substituted pyrrolo[2,3-*b*]pyridine-1-carboxamides (7-azaindoles) (**1**) were designed. These compounds incorporate a nitrogen atom into the aromatic ring to lock the N-carboxamide group within a six-membered 'pseudo-cycle' through an intramolecular hydrogen bond. The hypothesis that this interaction constrains the group into the

optimal binding orientation was supported by molecular modeling studies (see later). On the basis of these studies, a number of derivatives substituted in position 6 with aromatic or heterocyclic groups were designed and synthesized.

To the best of our knowledge, the 7-azaindoles structure represents a new scaffold for PARP inhibitors.

2. Results and discussion

2.1. Chemistry

Unsubstituted 7-azaindoles (**1a**) was obtained by reacting 7-azaindoles with triphosgene, followed by NH_3 treatment in CH_2Cl_2 (Scheme 1).

The 6-substituted derivatives were synthesized by regioselective substitution²¹ of 7-azaindoles N-oxide (**3**), in turn obtained by oxidation of 7-azaindoles with MCBA. Treatment of **3** with benzoyl bromide in anhydrous toluene in the presence of hexamethyldisilazane (HMDS) gave **4** in 71% yield. The acyl group on N-1 atom was readily removed by basic treatment to give 6-bromo-7-azaindoles (**5**) in 90% yield. Coupling with appropriate boronic acids via Pd/catalyzed Suzuki reactions allowed to introduce different aromatic and heteroaromatic rings at position 6. Finally, the carboxamide group was installed by treatment with triphosgene, followed by NH_3 .²² The yields of this last step were generally quite low (Scheme 1).

Given the low solubility of the prototype **1a**, further efforts concentrated on the addition of polar groups such as basic amines in order to improve the solubility of these lipophilic compounds. Unexpectedly, the reaction with triphosgene/ NH_3 on derivatives bearing at the distal *para*-position a morpholinomethyl or a piperidinomethyl group failed.

On the basis of these results, an exploration of alternative methods for the introduction of the carboxamide group was undertaken. Azaindoles **1g**, **1h**, **1j**, **1k**, were obtained by treatment of compounds **6g**, **6h**, **6j**, **6k** with 4-nitrophenylchloroformate to give the corresponding

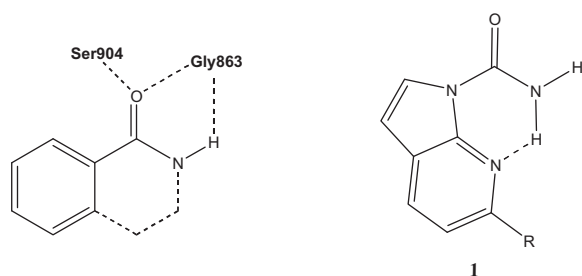
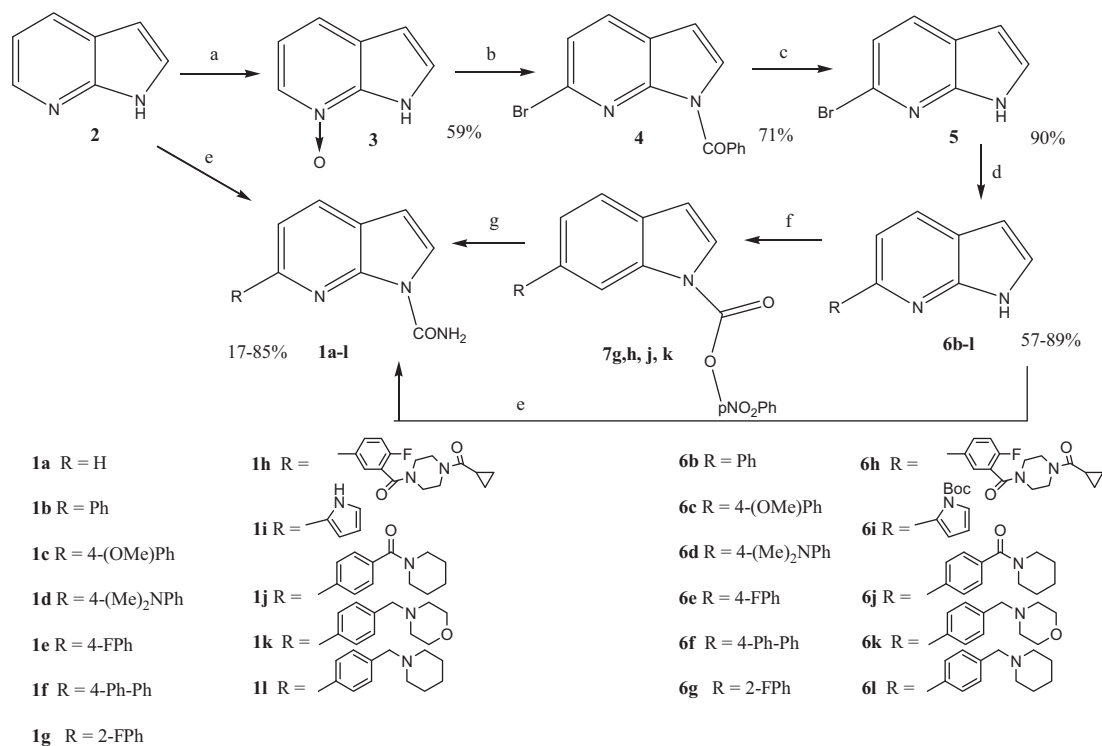


Figure 2. Scheme of the locked conformation of a PARP inhibitor in the nicotinamide binding pocket and structure of pyrrolo[2,3-*b*]pyridine-1-carboxamides (7-azaindoles) **1**.



Scheme 1. Reagents and conditions: (a) MCPBA, K₂CO₃, H₂O, rt; (b) PhCOBr, HMDS, toluene, N₂, rt, 1 h; (c) NaOH 1 N, MeOH, rt, overnight; (d) RB(OH)₂, PdCl₂(dppf)CH₂Cl₂, DME/H₂O 3.5:1, NaHCO₃, 110–115 °C; for **6f**: PdCl₂(dppf)CH₂Cl₂, 4-Br-biphenyl, bispinacolate diboron, KOAc, dioxane, 100 °C, 4 h, then **5**, PdCl₂(dppf)CH₂Cl₂, 2 M Na₂CO₃, 100 °C, 4 h; for **6h**: 3-carboxy-4-fluorophenylboronic acid, PdCl₂(dppf)CH₂Cl₂, DME/H₂O 3.5:1, NaHCO₃, 110–115 °C, then WSC, HOBT, DIPEA, 1-cyclopropylcarbonylpiperazine, DMF N₂, rt, 20 h; for **6i**: RB(OH)₂, K₂CO₃, Pd(Ph₃)₄, DME/H₂O 4:1, N₂, 100 °C, 3 h; (e) triphosgene, DIPEA, toluene, 80 °C, then NH₃; for **1a**: **2**, triphosgene, DIPEA, DCM, 0 °C, then NH₃; for **1i**: triphosgene, DIPEA, toluene, 80 °C, then NH₃, then MeOH/HCl, reflux, 5 h; for **1l**: LiHMDS, 4-nitrophenylchloroformate, THF, –78 °C, then NH₄Cl; (f) 4-nitrophenylchloroformate, Bu₄NBr, NaOH, toluene or DCM; (g) (NH₄)₂CO₃, DMF, 40 °C.

4-nitrophenylcarbamates.²³ The addition of ammonium carbonate gave the desired carboxamides. Unfortunately, when the same pathway was followed to obtain the aminoderivative **1l** the yield dropped to 17%.

Another synthetic route was then devised, in which the two final steps, that is Suzuki coupling and urea formation, were reversed. 7-Azaindole-1-carboxamide was obtained in overall quantitative yield by treatment of **5** with 4-nitrophenylchloroformate, followed by ammonium carbonate. Suzuki coupling with two different amino-containing boronic acids gave the desired compounds **1m**, **1n** together with consistent amounts of undesired hydrolysis derivatives, whose separation by flash chromatography resulted quite troublesome (Scheme 2).

In an attempt to overcome this problem, the carboxamide was protected as PMB²⁴ before Suzuki coupling and the protecting group was removed in the last step. The sequence was followed to synthesize compound **1o**, whose preparation by the previously reported methods failed (Scheme 3).

In an effort to evaluate the role of the urea group, a methylene spacer was introduced between the azaindole core and the carboxamide group. Treatment of compound **5** with iodoacetamide and final Suzuki coupling gave compound **11**, in 25% overall yield (Scheme 2).

To synthesize derivatives with a heterocyclic amine at position 6, 7-azaindole **2** was reacted with MCPBA followed by dimethyl sulfate in acetonitrile and suitable amines to give the derivatives **6p–r**.²⁵ Treatment with triphosgene or 4-nitrophenylchloroformate, followed by quenching with ammonium carbonate, afforded the corresponding carboxamides **1p–r** (Scheme 4).

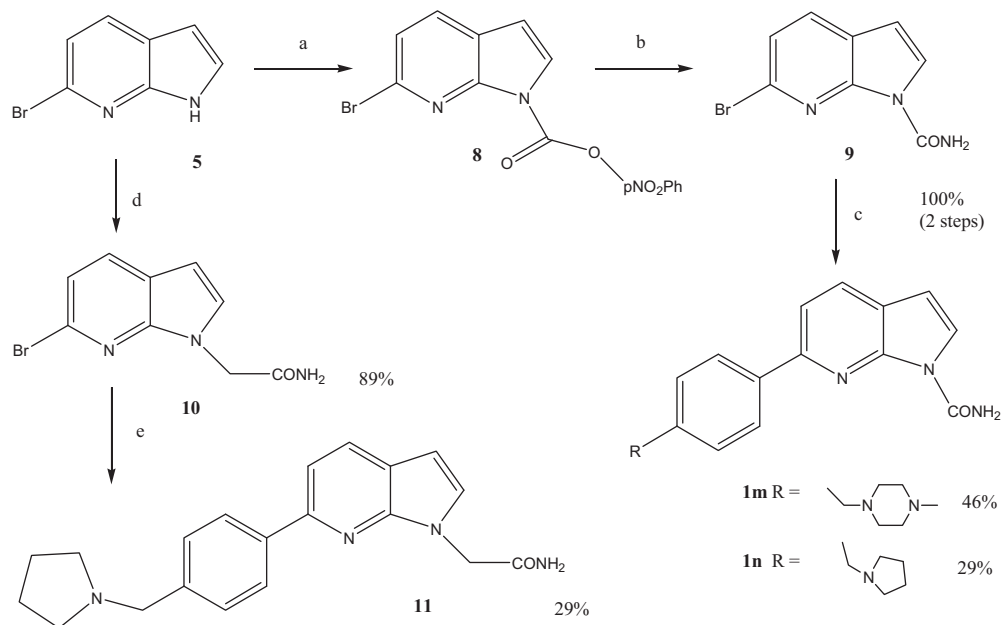
On the basis of biological activity results (see later) derivative **1l** was selected for further in vitro and in vivo investigation. As it was

initially obtained in very low yield, the synthetic strategy was revised in the light of the various attempts made to install the troublesome N-carboxamide group. After extensive experimentation, the compound was prepared by the sequence reported in Scheme 5. Protection of the carboxamide with one PMB group was accomplished reacting *p*-methoxybenzylamine with isopropenyl chloroformate to give the corresponding isopropenyl carbamate **17**.²⁶ This procedure showed to be very advantageous because it afforded urea **18** in high yield in a single step from 6-bromoazaindole. Moreover, the use of isopropenyl chloroformate instead of 4-nitrophenylchloroformate avoided the formation of 4-nitrophenol as a side product and gave a crude that was easily purified, as the acetone formed was removed by evaporation. Suzuki coupling, followed by deprotection in TFA at reflux gave **11** in good yield. This procedure affording the compound on a multi-gram scale can be considered a convenient and rapid method to synthesize 6-substituted pyrrolo[2,3-*b*]pyridine-1-carboxamides (7-azaindole-1-carboxamides) in high yield and high purity.

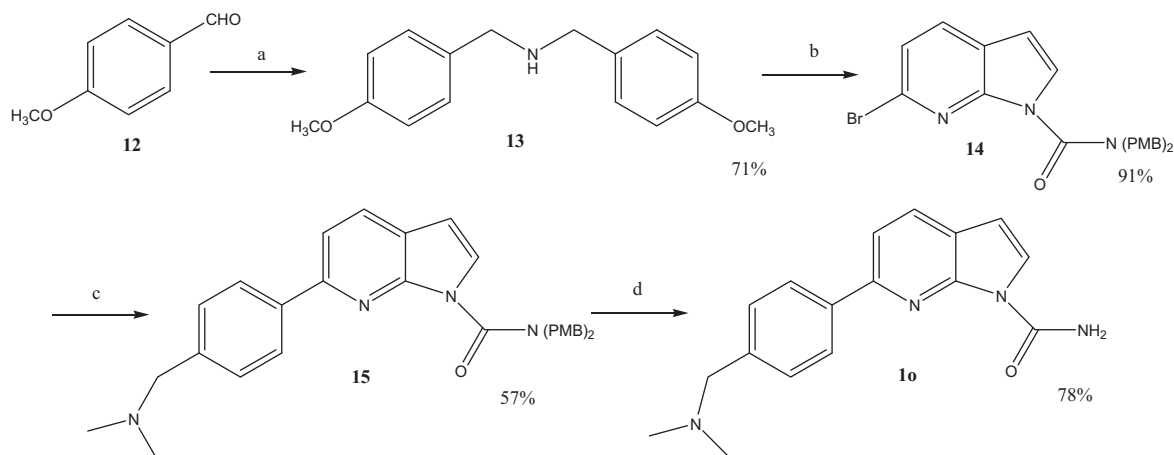
2.2. PARP-1 inhibitory activity

The compounds prepared in this study were evaluated for their inhibitory activity against recombinant human PARP-1, expressed as GST fusion protein, by means of a highly sensitive fluorescent enzymatic assay. The results are summarized in Table 1. Three PARP inhibitors—Olaparib,²⁷ ABT-888¹⁹ and MK-427²⁸—were included for comparative purposes.

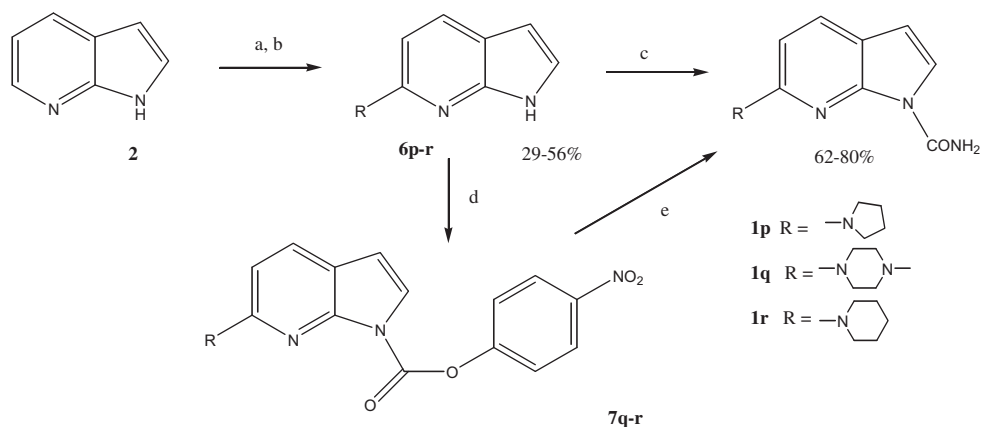
The novel scaffold prototype **1a** showed an encouraging activity as PARP-1 inhibitor, displaying an IC₅₀ value of 2.5 μM. Therefore, a more detailed exploration of the 7-azaindole-1-carboxamide scaffold was undertaken. In an effort to improve the activity,



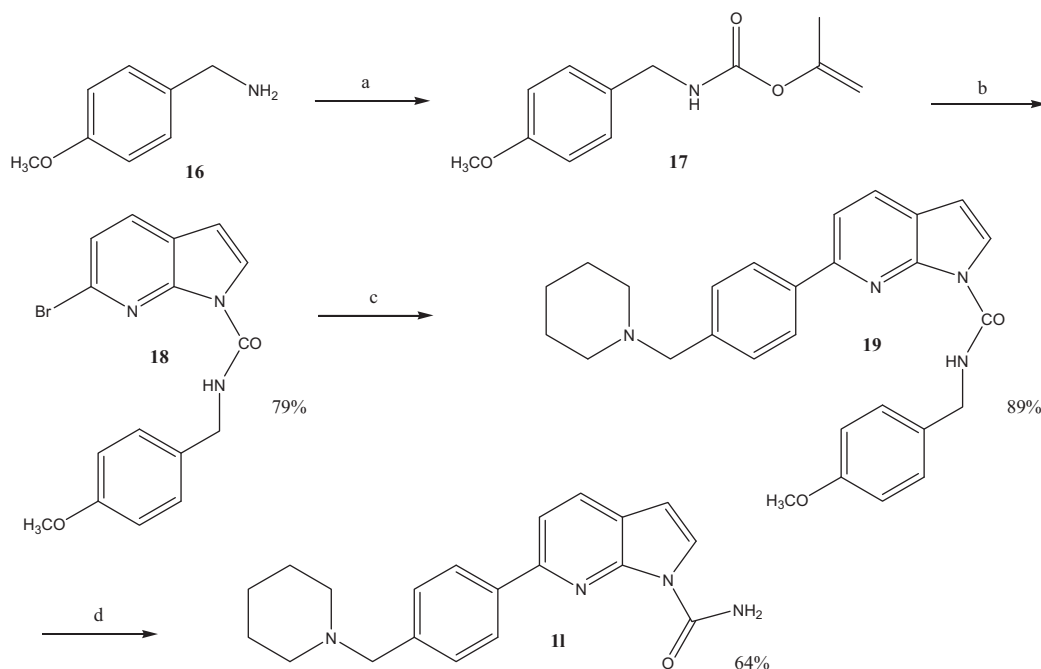
Scheme 2. Reagents and conditions: (a) 4-nitrophenylchloroformate, Bu_4NBr , NaOH, DCM; (b) $(\text{NH}_4)_2\text{CO}_3$, DMF, 40 °C; (c) RB(OH)_2 , $\text{PdCl}_2(\text{dppf})\text{CH}_2\text{Cl}_2$, DME/ H_2O 3.5:1, NaHCO_3 , 80–110 °C; (d) NaH, DMF, 0 °C, iodoacetamide; (e) $\text{PdCl}_2(\text{dppf})\text{CH}_2\text{Cl}_2$, DME/ H_2O 3.5:1, NaHCO_3 , 110 °C.



Scheme 3. Reagents and conditions: (a) 4-methoxybenzylamine, EtOH, reflux, 9 h, then NaBH_4 , MeOH; (b) **8**, anhydrous DMF, 60 °C, 6 h; (c) pinacol 4[(*N,N*-dimethylamino)methyl]phenylboronate-HCl, $\text{PdCl}_2(\text{dppf})\text{CH}_2\text{Cl}_2$, NaHCO_3 , DME/ H_2O ; 100 °C, 3 h; (d) TFA, reflux, 9 h.



Scheme 4. Reagents and conditions: (a) MCPBA, DME, rt; (b) Me_2SO_4 , base, 50–55 °C, MeCN; (c) triphosgene, DIPEA, toluene, 80 °C, then NH_3 ; (d) 4-nitrophenylchloroformate, Bu_4NBr , NaOH, toluene, reflux; (e) $(\text{NH}_4)_2\text{CO}_3$, DMF, 45 °C.



Scheme 5. Reagents and conditions: (a) NaOH, H₂O, AcOEt, isopropenyl chloroformate, rt, 3 h; (b) NaH, **5**, rt, 20 h; (c) PdCl₂(dppf)CH₂Cl₂, NaHCO₃, DME/H₂O 3.5: 1, reflux, 45 min; (d) TFA, CH₂Cl₂, reflux, 34 h.

substituents were introduced at position 6 of the azaindole system. As the introduction of a phenyl moiety resulted in a ten-fold increase of activity (**1b**, IC₅₀ = 0.27 μM), variously substituted aromatic rings were linked to carbon 6 (compounds **1c–h**). In general, these compounds showed good inhibitory activity, comparable to that of **1b**, with IC₅₀ values ranging from 0.27 to 1.12 μM. The introduction of an *ortho*-substituted aromatic ring (compound **1g**) led to a decrease in the inhibitory activity (IC₅₀ = 3 μM). The introduction of a further phenyl ring (compound **1f**) was also detrimental, resulting in complete loss of the enzymatic activity (no activity up to 5 μM).

Successively, aliphatic aminomethyl groups were added at *para* position of the phenyl ring (compounds **1k, l**), with the aim of improving solubility and picking up additional interactions in the adenosine binding pocket. Both compounds retained a significant activity against the enzyme, with **1l** displaying IC₅₀ = 0.07 μM. The introduction of an amido group in place of the amino group (**1j** vs **1l**) led to a decrease of activity.

The insertion of a methylene spacer between the azaindole core and the carboxamide moiety (**1n** vs **1l**) resulted in a loss of enzymatic activity, thus confirming the crucial role of the nitrogen-linked carboxamido group.

The effect of the distance between the basic amine and the core scaffold was also investigated. Accordingly, compounds **1p–r** were prepared by directly linking the amine nitrogen to the azaindole nucleus. Whereas compounds **1p–q** maintained a good activity, **1r** showed a decrease in inhibitory activity (IC₅₀ = 3 μM).

2.3. Molecular modelling studies

The orientations of the described systems inside the binding site were obtained by using molecular docking experiments that were further optimised using the QM/MM mixed approach on the resulting complexes. This QM/MM mixed approach allowed us to obtain a more complete description of the interactions of the studied compounds with the human PARP-1 system, as well as an estimate of the structural changes induced in the complex

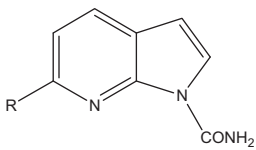
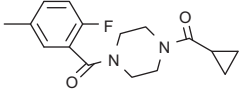
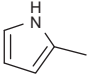
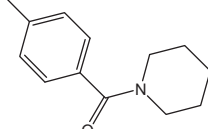
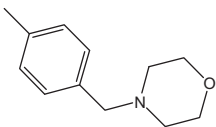
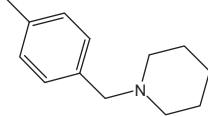
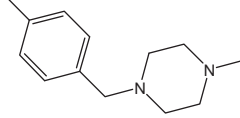
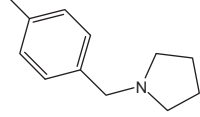
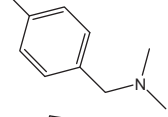
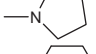
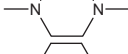
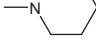
by the binding of the ligands (induced fit). All the examined structures were bound in the nicotinamide binding site in a very similar way, with the azaindole ring inserted between the Y246 and H201 residues, interacting with Y246 through a strong π -stacking interaction, with a distance between the centers of mass of the two rings equal to 3.81 Å for **1l**. As planned, the carboxamide group forming the 'pseudo-cycle' gives rise to three hydrogen bonds: one with the S243 hydroxyl (1.91 Å) and two with the G202 backbone (1.82 and 2.03 Å with NG202 and OG202, respectively). Considering the most active product (**1l**, Fig. 3), the pattern of interaction with PARP-1 is completed by a hydrogen bond between the charged nitrogen of the piperidine ring and the hydroxyl group of Y228, with a distance of 2.04 Å.

The possibility to interact with the Y228 residue is a feature accessible by those compounds (like e.g., **1l** and **1n**) with a charged residue extending within the binding site of the enzyme, toward the external loops, contributing to increase the affinity of these ligands. This interaction becomes clearly impossible in cases where the side chain is too short (e.g., **1p** and **1c**) or conformationally too much constrained (e.g., **1f**) to reach the external loops, or when the compound lacks charged substituents (like **1c**). In these cases the compounds (although correctly inserted) are not able to interact optimally with the residues of the binding site, as shown in Figure 4 for compounds **1c**, **1f** and **1p**. In this latter case the contribution of some water molecules present in the binding site may explain the relative good affinity with the enzyme, a contribution which, however, was not taken into account in this study.

2.4. Sensitivity of BRCA1/2 defective tumor cell lines to PARP inhibitors

PARP inhibitors were tested in vitro for their antiproliferative activity and compared to the reference compounds Olaparib and ABT 888 against human tumor cell lines HCC1937 and Capan 1, characterized by BRCA1 and BRCA2 gene mutation, respectively. The cell sensitivity assays (Table 2) indicated that compounds

Table 1
Inhibitory activity of synthesized compounds against recombinant human PARP-1

		
Compd	R	PARP-1 activity (enzymatic assay) IC ₅₀ (μM)
Olaparib		0.0045
MK-4827		0.0323
ABT-888		0.0052
1a	H	2.5
1b	Ph	0.27
1c	4-(OCH ₃)Ph	3.76
1d	4-(CH ₃) ₂ NPh	0.88
1e	4-FPh	0.27
1f	4-PhPh	>5
1g	2-FPh	3.0
1h		1.12
1i		0.93
1j		2.9
1k		2.10
1l		0.07
1m		1.56
1n		0.28
1o		0.63
1p		0.22
1q		0.77
1r		3.00
11		>5

1a–f and **1p** were inactive in HCC1937 cells, as no inhibition of proliferation was observed up to 200 μM drug concentration. In the HCC1937 cell line, the most promising compounds in terms of

proliferation inhibition appeared to be **1k**, **1l**, **1n**, and **1o**, the IC₅₀ values being around 10–20 μM. Compounds **1a**, **1b** and **1d** were inactive also in Capan 1 cells, meanwhile compound **1c**, **1e** and

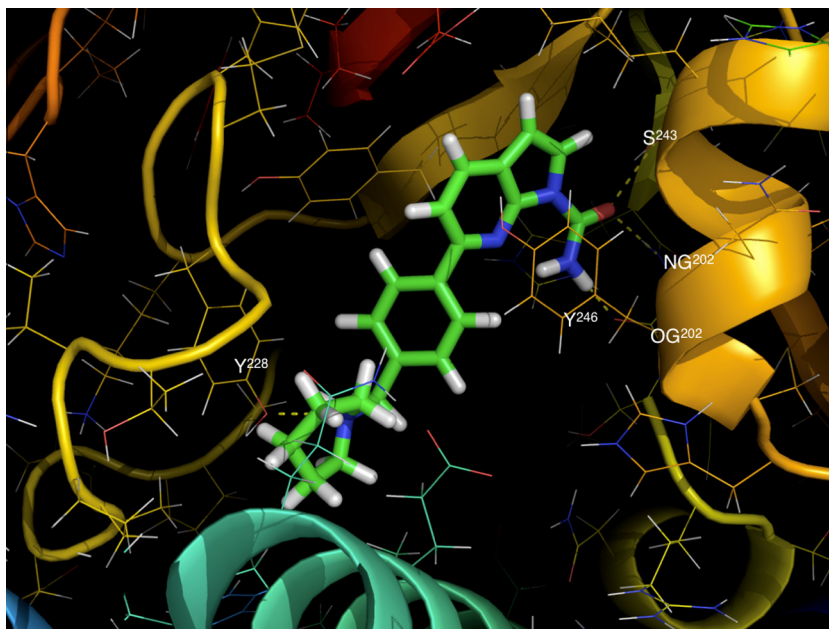


Figure 3. Representation of **1l** binding mode with the key residues highlighted. Ligand is represented as stick and coloured by atoms. PARP-1 residues are rendered in wireframe.

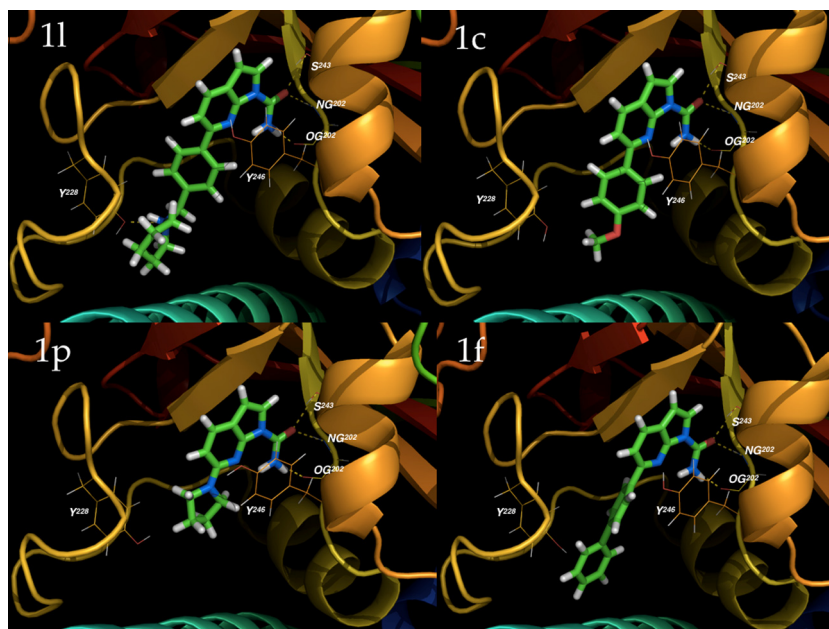


Figure 4. Representation of **1l**, **1c**, **1p** and **1f** binding modes with the key residues highlighted. Ligands are represented as stick and coloured by atoms. PARP-1 residues are rendered in wireframe.

1f displayed a poor antiproliferative activity. In both cell lines, the antiproliferative effect of **1k**, **1l**, **1n** and **1o** was in the range of 20 μ M. The antiproliferative activity of such compounds was lower than that of Olaparib but higher than that of ABT-888. Therefore, given cell sensitivity data and the profile of PARP inhibition we focused on compound **1l** for further studies.

Cell sensitivity to compound **1l** was also evaluated on the ovarian carcinoma parental A2780 cells and on the drug-resistant variant A2780/Dx characterized by a multidrug-resistant phenotype associated to overexpression of *P*-glycoprotein (Pgp) (Table 3). In drug resistant cells a slightly reduced sensitivity to compound **1l** was observed as compared to parental cells, the resistance index

being around 4. Since a marked resistance of the A2780/Dx cells to Olaparib was observed (resistance index around 40), compound **1l** appears to be poorly recognized by Pgp. The activity of the compound on multi-drug resistant cells is a promising feature supporting further development of such a PARP inhibitor.

2.5. Assessment of the inhibitory activity on a cellular PARylation assay

Compound **1l** showed to be an active inhibitor also through a functional PARylation assay on a cellular model (HeLa human endometrial carcinoma cell line). HeLa cells are usually used for

Table 2
Cell sensitivity of cells with BRCA1 (HCC1937) and BRCA2 (Capan 1) gene mutations^a

Compd	HCC1937; IC ₅₀ (μM ± SD)	Capan 1; IC ₅₀ (μM ± SD)
Olaparib	10.3 ± 5.4	6.3 ± 2.5
ABT-888	97.16 ± 32	39.7 ± 4.7
1a	>200	>200
1b	>200	>200
1c	>200	161.9 ± 35.1
1d	>200	>200
1e	>200	61.1 ± 19.6
1f	>200	81.8 ± 1.9
1g	n.d.	n.d.
1h	n.d.	n.d.
1i	61.43 ± 15.02	87.07 ± 42.9
1j	72.33 ± 18.9	24.4 ± 12.0
1k	17.24 ± 4.4	15.90 ± 8.9
1l	19.43 ± 4.2	22.04 ± 9.2
1m	41.21 ± 4.9	54.52 ± 22.9
1n	14.98 ± 1.56	21.69 ± 5.9
1o	13.45 ± 3.0	19.71 ± 11.9
1p	>200	83.8 ± 7.8
1q	110.67 ± 43.3	138.4 ± 27.0
1r	n.d.	n.d.
11	182.4 ± 4.2	182.4 ± 4.2

^a Cell sensitivity was evaluated by growth inhibition assays based on cell counting. Cells were seeded and 24 h later they were exposed to the compounds for 72 h. At the end of treatment, cells were counted using a cell counter.

Table 3
Cell sensitivity to compound **11** and Olaparib of cell lines overexpressing Pgp^a

Compd	A2780 ovarian ca.	A2780/Dx (Pgp) ovarian ca.	Resistance index
		IC ₅₀ , μM	
Olaparib	1.00	41.9	41.9
11	2.90	11.2	3.9

^a Cell sensitivity was evaluated after 72 h exposure. Results are expressed as IC₅₀ (μM), and the relative standard deviations were lower than 10%. Resistance index is the ratio between IC₅₀ of resistant and sensitive cells.

this functional assay because they represent the most suitable model to measure, in a simple and efficient way, the ability of tested compounds to affect the PARP-mediated PARylation of nuclear proteins, following a strong DNA damage induced by treatment with H₂O₂.²⁹

As shown in Figure 5, the extent of PARylated proteins decreased in a dose-dependent manner in cells pre-treated with compound **11**, although to lesser extent (EC₅₀ = 400 nM) with respect to Olaparib (EC₅₀ = 2.5 nM), as expected on the basis of their relative activity against recombinant PARP-1 enzyme (Table 1). Only very marginal fluorescent signals were measured at the highest dose, thus confirming the ability of compound **11** to target and inhibit PARP-1 activity.

2.6. Evaluation of in vivo antitumor activity

Antitumor activity of compound **11**, delivered i.p. and administered every 2 days for 2 weeks (qd2/wx2w), was examined on the in vivo breast carcinoma line MX1, a triple-negative human breast tumor carrying BRCA1 deletion and BRCA2 mutation, that grows in athymic (SCID beige) mice as subcutaneous (s.c.) tumor.

A significant antitumor effect was observed following administration of a dose 100 mg/kg of compound **11** (Table 4). When compared to Olaparib (167 mg/kg) administered with the same schedule, compound **11** displayed a similar effect in terms of tumor volume inhibition (TVI, around 35%). Treatment was well tolerated, as no deaths or significant weight losses were observed among the treated animals.

3. Conclusions

In conclusion, we have synthesized a series of 6-substituted pyrrolo[2,3-*b*]pyridine-1-carboxamides (7-azaindoles) in which the pyridine- nitrogen atom locks the N-carboxamide group within a six-membered 'pseudo-cycle' through an intramolecular hydrogen bond. Molecular modelling studies support that this interaction constrains the group into the optimal binding orientation. The generation of 6-substituted derivatives with aromatic or heterocyclic groups allowed us to identify the 7-azaindole as a new scaffold for PARP inhibition.

The compounds displayed a variable pattern of target inhibition profile that in part paralleled the antiproliferative activity in cell lines characterized by homologous recombination defects.

Among the compounds, the promising features of **11** (ST7710AA1), emerged based on in vitro target inhibition, cell sensitivity and capability to substantially bypass the multidrug resistance mediated by Pgp. In antitumor activity studies against the MX1 human breast carcinoma growth in nude mice, compound **11** exhibited an effect similar to that of Olaparib in terms of tumor volume inhibition when used at a lower dose than the reference compound. Treatment was well tolerated, as no deaths or significant weight losses were observed among the treated animals.

All these results suggest that 7-azaindole-1-carboxamides can be considered a new series of PARP-1 inhibitors with potent in vitro and in vivo activity, which are worth of further development toward a candidate for tumor treatment.

4. Experimental section

4.1. General experimental method

All reagents and solvents were reagent grade or were purified by standard methods before use. Melting points were determined in open capillaries and are uncorrected. NMR spectra were recorded at 300 MHz. Chemical shifts (δ values) and coupling constants (*J* values) are given in ppm and Hz, respectively. Solvents were routinely distilled prior to use; anhydrous tetrahydrofuran (THF) and ether (Et₂O) were obtained by distillation from sodium-benzophenone ketyl; dry methylene chloride was obtained by distillation from phosphorus pentoxide. All reactions requiring anhydrous conditions were performed under a positive nitrogen flow, and all glassware were oven dried and/or flame dried. Isolation and purification of the compounds were performed by flash column chromatography on silica gel 60 (230–400 mesh). Analytical thin-layer chromatography (TLC) was conducted on Fluka TLC plates (silica gel 60 F₂₅₄, aluminum foil).

Compounds **3**,³⁰ **4**²¹ and **5**²¹ were synthesized according to literature procedures.

4.2. Pyrrolo[2,3-*b*]pyridine-1-carboxylic acid amide (**1a**)

To a solution of triphosgene (503 mg, 1.70 mmol) in dichloromethane (5 mL) cooled to 0 °C compound **2** (500 mg, 4.23 mmol) dissolved in dichloromethane (10 mL), DIPEA (1.6 mL, 9.30 mmol) and NH₃/CH₂Cl₂ (5 mL saturated solution) were dropped sequentially. The mixture was stirred at room temperature for 2 h, then it was washed twice with 0.25 M HCl, twice with saturated NaHCO₃ solution, then dried and evaporated. The residue was purified by flash chromatography (CH₂Cl₂: acetone 99:1) to obtain the title compound as a white solid. Yield 20%; mp 169 °C; ¹H NMR (CDCl₃) δ 9.68 (1H, br s); 8.33 (1H, dd, *J* = 4.9, 1.8 Hz); 8.00 (1H, d, *J* = 3.7 Hz); 7.95 (1H, dd, *J* = 8.2, 1.8 Hz); 7.23 (1H, dd, *J* = 8.2, 4.9 Hz); 6.59 (1H, d, *J* = 3.7 Hz); 5.55 (1H, br s).

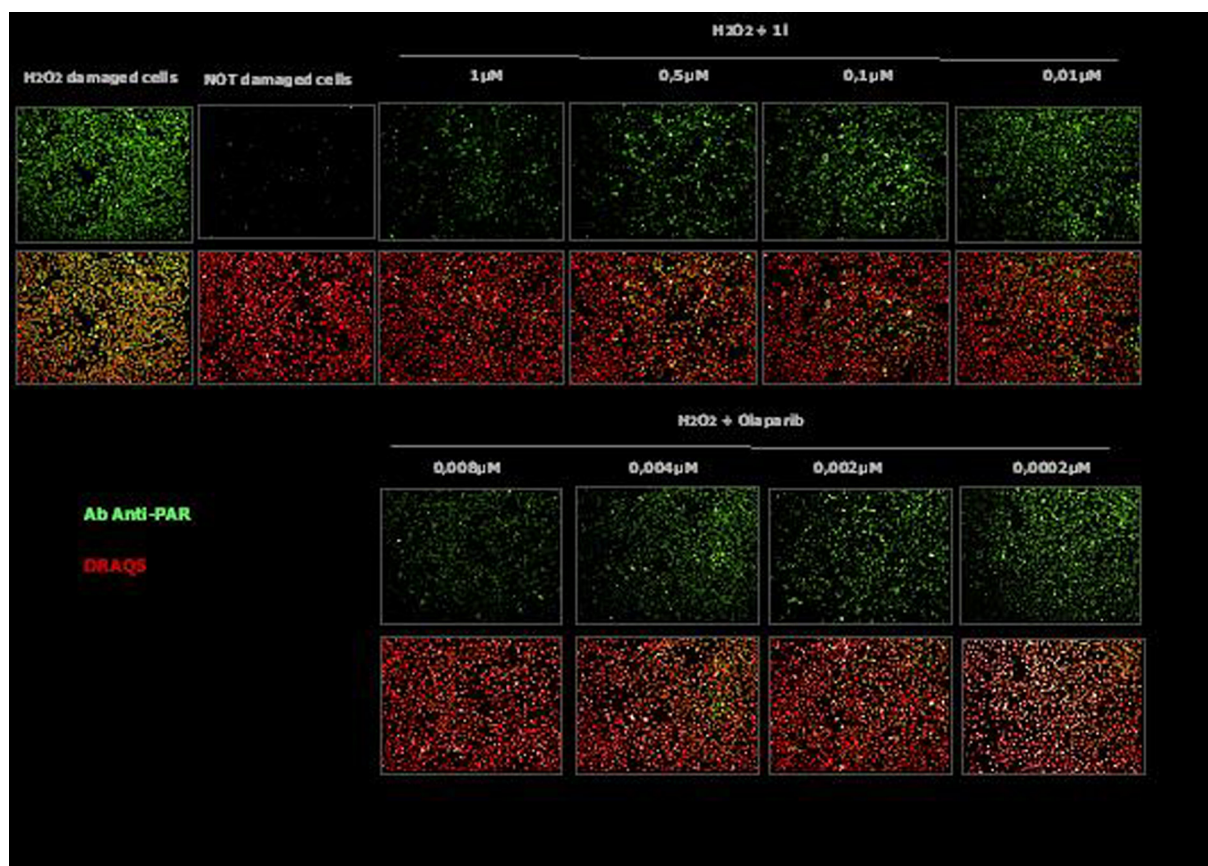


Figure 5. Effect of **11** and Olaparib on nuclear protein PARylation in HeLa (human endometrial ca.) cells. Cells were pre-treated with serial dilutions of test compounds for 18 h at 37 °C. DNA damage was then provoked by addition of H₂O₂ 500 μM. As negative control, cells untreated with H₂O₂ were used. Protein PARylation was detected in fixed cells by using the primary PAR mAb (Alexis) and the secondary anti-mouse Alexa Fluor 488 antibody (Molecular probes). Fluorescence signals, related to the residual amount of PAR polymer on nuclear proteins, were read on the HCS system Operetta. Nuclei were stained with 5 μM Draq5 (Alexis). The percent of PAR-positive cells was calculated at last by measuring the ratio between the numbers of PAR-positive nuclei over the total number of Draq5-labeled nuclei.

Table 4

Antitumor activity of **11** in comparison with Olaparib against MX1 breast carcinoma

Compd	Dose/route; mg/kg	Schedule	BWL %	Lethality	TV ± SE (d + 38)	TVI % (d + 38)
Vehicle	0	q2d/wx2w	0	0/8	781 ± 296	
11	100/ip	q2d/wx2w	1	0/8	502 ± 32	*36
Olaparib	167ip	q2d/wx2w	0	0/8	511 ± 64	*35

Treatments started 7 days after tumor injection.

* $P < 0.05$ versus vehicle-treated group (Mann–Whitney's test).

Anal. Calcd for C₈H₇N₃O: C, 59.62; H, 4.38; N, 26.07. Found: C, 59.75; H, 4.42; N, 26.17.

4.3. Suzuki–Miyaura reactions. General procedure A³¹

To a degassed 3.5:1 mixture of dimethoxyethane and water (2 mL), compound **5** (0.5 mmol), the appropriate boronic acid (1 mmol), PdCl₂(dppf)CH₂Cl₂ (0.025 mmol) and sodium bicarbonate (1.5 mmol) were added under nitrogen. The mixture was heated for 1–4 h. The layers were separated and the organic phase was evaporated. Purification by flash chromatography gave the desired compounds. Following this procedure compounds **1m–n**, **6b–e**, **6g–h**, **6j**, **6l–m**, **11**, **15** were prepared.

4.3.1. 6-[4-(4-Methyl-piperazin-1-ylmethyl)-phenyl]-pyrrolo[2,3-*b*]pyridine-1-carboxylic acid amide (**1m**)

From compound **9**. Heated 3.5 h at 80 °C. Flash chromatography (CH₂Cl₂:MeOH 92:8). Yield 46%; white solid; mp 151 °C; ¹H NMR (CDCl₃) δ 9.80 (1H, br s); 8.05–7.97 (2H, m); 7.93 (2H, d,

$J = 8.2$ Hz); 7.65 (1H, d, $J = 8.1$ Hz); 7.50–7.37 (2H, m); 6.60 (1H, d, $J = 3.8$ Hz); 5.63 (1H, br s); 3.73–3.63 (2H, m), 2.99–2.81 (8H, m); 2.70 (3H, br s). Anal. Calcd for C₂₀H₂₃N₅O: C, 68.74; H, 6.63; N, 20.04. Found: C, 69.00; H, 6.65; N, 20.07.

4.3.2. 6-(4-Pyrrolidin-1-ylmethyl-phenyl)-pyrrolo[2,3-*b*]pyridine-1-carboxylic acid amide (**1n**)

From compound **9**. Heated 1 h at 110 °C. Flash chromatography (CH₂Cl₂:MeOH 92:8). Yield 29%; white solid. mp 168 °C; ¹H NMR (CDCl₃) δ 9.73 (1H, br s); 8.04–7.94 (4H, m); 7.77 (2H, d, $J = 7.3$ Hz); 7.66 (1H, d, $J = 8.4$ Hz); 6.60 (1H, d, $J = 3.4$ Hz); 5.63 (1H, br s); 4.17 (2H, s); 3.39–2.62 (4H, m); 2.33–2.12 (4H, m). Anal. Calcd for C₁₉H₂₀N₄O: C, 71.23; H, 6.29; N, 17.49. Found: C, 71.35; H, 6.27; N, 17.42.

4.3.3. 6-Phenyl-1H-pyrrolo[2,3-*b*]pyridine (**6b**)

Heated 2 h at 110–115 °C. Purification by flash chromatography (hexane: ethyl acetate 9:1). Yield 58%; white solid; mp 136 °C; ¹H NMR (DMSO-*d*₆) δ 11.70 (1H, br s), 8.09 (2H, d, $J = 7.4$ Hz); 8.03 (1H,

d, $J = 8.2$ Hz); 7.65 (1H, d, $J = 8.2$ Hz); 7.53–7.44 (3H, m); 7.38 (1H, m); 6.47 (1H, m). Anal. Calcd for $C_{13}H_{10}N_2$: C, 80.39; H, 5.19; N, 14.42. Found: C, 80.44; H, 5.21; N, 14.36.

4.3.4. 6-(4-Methoxyphenyl)-1H-pyrrolo[2,3-*b*]pyridine (6c)

Heated 2 h at 110–115 °C. Purification by flash chromatography (hexane:ethyl acetate 7:3). Yield 85%; white solid; mp 185 °C; 1H NMR ($CDCl_3$) δ 10.22 (1H, br s); 8.01 (1H, d, $J = 7.8$ Hz); 7.99 (2H, d, $J = 8.7$ Hz); 7.51 (1H, d, $J = 7.8$ Hz); 7.26 (1H, m); 7.06 (2H, d, $J = 8.7$ Hz); 6.52 (1H, m); 3.91 (3H, s). Anal. Calcd for $C_{14}H_{12}N_2O$: C, 74.98; H, 5.39; N, 12.49. Found: C, 75.11; H, 5.32; N, 12.53.

4.3.5. Dimethyl-[4-(1H-pyrrolo[2,3-*b*]pyridin-6-yl)phenyl]-amine (6d)

Heated 90 min at 110–115 °C. Purification by flash chromatography (hexane:ethyl acetate 7:3). Yield 64%; white solid; mp 198 °C; 1H NMR ($DMSO-d_6$) δ 11.61 (1H, br s); 8.02 (1H, d, $J = 8.7$ Hz); 7.96 (2H, d, $J = 8.4$ Hz); 7.57 (1H, d, $J = 8.7$ Hz); 7.41 (1H, m); 6.89 (2H, d, $J = 8.4$ Hz); 6.44 (1H, m); 2.98 (6H, s). Anal. Calcd for $C_{15}H_{15}N_3$: C, 75.92; H, 6.37; N, 17.71. Found: C, 75.80; H, 6.31; N, 17.96.

4.3.6. 6-(4-Fluorophenyl)-1H-pyrrolo[2,3-*b*]pyridine (6e)

Heated 90 min at 110–115 °C. Purification by flash chromatography (hexane:ethyl acetate 8:2). Yield 82%; white solid; mp 216 °C; 1H NMR ($CDCl_3$) δ 10.63 (1H, br s); 8.08–7.94 (3H, m); 7.49 (1H, d, $J = 8.2$ Hz); 7.27–7.14 (3H, m); 6.52 (1H, m). Anal. Calcd for $C_{13}H_9FN_2$: C, 73.57; H, 4.27; N, 13.20. Found: C, 73.79; H, 4.23; N, 13.44.

4.3.7. 6-(2-Fluorophenyl)-1H-pyrrolo[2,3-*b*]pyridine (6g)

Heated 1 h at 110–115 °C. Purification by flash chromatography (hexane:ethyl acetate 7:3). Yield 78%; white solid; mp 155 °C; 1H NMR ($CDCl_3$) δ 11.24 (1H, br s); 8.03 (1H, d, $J = 8.2$ Hz); 7.93 (1H, t, $J = 7.5$ Hz); 7.54 (1H, dd, $J = 1.9$; 8.1 Hz); 7.42 (1H, m); 7.37–7.15 (3H, m); 6.50 (1H, m). Anal. Calcd for $C_{13}H_9FN_2$: C, 73.57; H, 4.27; N, 13.20. Found: C, 73.79; H, 4.22; N, 13.48.

4.3.8. (4-Cyclopropanecarbonylpiperazin-1-yl)-[2-fluoro-5-(1H-pyrrolo[2,3-*b*]pyridin-6-yl)-phenyl]-methanone (6h)

To a solution of **5** (100 mg, 0.51 mmol) in degassed DME/ H_2O 3.5:1 (2 mL) under N_2 were added 3-carboxy-4-fluorophenylboronic acid (188 mg, 1.02 mmol), $NaHCO_3$ (128 mg, 1.53 mmol) and $PdCl_2(dppf)CH_2Cl_2$ (19 mg, 0.025 mmol). The solution was heated for 2 h at 80 °C and for 2 h at 110 °C in the dark. After addition of ethyl acetate, the mixture was washed with 1 N HCl. The aqueous phase was extracted three times with ethyl acetate. The collected organic layers were dried, filtered and evaporated to give a crude (252 mg) that was suspended in CH_2Cl_2 (10 mL) and methanol (0.5 mL). The resulting mixture was refluxed for 30 min., cooled and filtered to give 2-fluoro-5-(1H-pyrrolo[2,3-*b*]pyridin-6-yl)-benzoic acid as a pale yellow sticky solid (70 mg, 54%); 1H NMR ($DMSO-d_6$) δ 11.78 (1H, br s); 8.67 (1H, dd, $J = 2.0$, 7.5 Hz); 8.33 (1H, m); 8.06 (1H, d, $J = 8.2$ Hz); 7.70 (1H, d, $J = 8.2$ Hz); 7.53 (1H, m); 7.41 (1H, m); 6.49 (1H, m).

To a solution of the above compound (68 mg, 0.27 mmol) in anhydrous DMF (2 mL) under N_2 at 0 °C were added WSC (61 mg, 0.32 mmol) and HOBt (43 mg, 0.32 mmol). The resulting mixture was stirred for 30 min, then it was added with DIPEA (141 μ L, 0.81 mmol) and 1-(cyclopropylcarbonyl)piperazine (115 μ L, 0.81 mmol). Stirring was continued at room temperature for 20 h. The residue was partitioned between water and ethyl acetate and the phases were separated. The organic layer was washed with brine, dried, filtered and evaporated. Purification by flash chromatography (CH_2Cl_2 :MeOH 95:5) afforded 85 mg (80%) of the title compound. 1H NMR ($CDCl_3$) δ 10.88 (1H, br s); 8.18–7.95 (3H,

m); 7.47 (1H, d, $J = 8.4$ Hz); 7.34–7.18 (2H, m); 6.50 (1H, m); 3.97–3.73 (4H, m); 3.88–3.72 (2H, m); 3.54–3.34 (2H, m); 1.75 (1H, m); 1.09–0.94 (2H, m); 0.90–0.64 (2H, m). Anal. Calcd for $C_{22}H_{21}FN_4O_2$: C, 67.33; H, 5.39; N, 14.28. Found: C, 69.86; H, 5.34; N, 13.88.

4.3.9. Piperidin-1-yl-[4-(1H-pyrrolo[2,3-*b*]pyridin-6-yl)-phenyl]-methanone (6j)

Heated 1 h at 110–115 °C. Purification by flash chromatography (CH_2Cl_2 :MeOH 97:3). Yield 89%; white solid; mp 183 °C; 1H NMR ($CDCl_3$) δ 10.64 (1H, br s); 8.11–7.97 (3H, m); 7.59–7.50 (3H, m); 7.25 (1H, m); 6.50 (1H, m); 3.86–3.66 (2H, m); 3.53–3.29 (2H, m); 1.78–1.41 (6H, m). Anal. Calcd for $C_{19}H_{19}N_3O$: C, 74.73; H, 6.27; N, 13.76. Found: C, 74.66; H, 6.22; N, 13.60.

4.3.10. 6-(4-Morpholin-4-ylmethyl-phenyl)-1H-pyrrolo[2,3-*b*]pyridine (6k)

Heated 1 h at 110 °C. Purification by flash chromatography (CH_2Cl_2 : MeOH 95:5). Yield 81%; white solid; mp 170 °C; 1H NMR ($CDCl_3$) δ 10.75 (1H, br s); 8.02 (1H, d, $J = 8.4$ Hz); 7.98 (2H, d, $J = 7.7$ Hz); 7.53 (1H, d, $J = 8.4$ Hz); 7.49 (2H, d, $J = 7.7$ Hz); 7.22 (1H, m); 6.50 (1H, m); 3.83–3.67 (4H, m); 3.61 (2H, s); 2.64–2.39 (4H, m). Anal. Calcd for $C_{18}H_{19}N_3O$: C, 73.69; H, 6.53; N, 14.32. Found: C, 73.51; H, 6.58; N, 14.12.

4.3.11. 6-(4-Piperidin-1-ylmethyl-phenyl)-1H-pyrrolo[2,3-*b*]pyridine (6l)

Heated 1 h at 110–115 °C. Purification by flash chromatography (CH_2Cl_2 : MeOH 92:8). Yield 68%; white solid; mp 190 °C; 1H NMR ($DMSO-d_6$) δ 11.66 (1H, br s); 8.07–7.92 (3H, m); 7.62 (1H, d, $J = 8.7$ Hz); 7.46 (1H, m); 7.37 (2H, d, $J = 8.2$ Hz); 6.44 (1H, m); 3.45 (2H, s); 2.42–2.27 (4H, m), 1.55–1.31 (6H, m).

Anal. Calcd for $C_{19}H_{21}N_3$: C, 78.32; H, 7.26; N, 14.42. Found: C, 78.49; H, 7.22; N, 14.66.

4.3.12. 2-[6-(4-Pyrrolidin-1-ylmethyl-phenyl)-pyrrolo[2,3-*b*]pyridin-1-yl]-acetamide (11)

From compound **10**. Heated 1 h at 110 °C. Crystallized from CH_2Cl_2 . Yield 29%; white solid; mp 181 °C; 1H NMR ($DMSO-d_6$) δ 8.11–7.93 (3H, s); 7.71–7.58 (2H, m); 7.51 (1H, d, $J = 3.0$ Hz); 7.40 (2H, d, $J = 7.6$ Hz); 7.23 (1H, br s); 6.48 (1H, d, $J = 3.0$ Hz); 4.95 (2H, s); 3.61 (2H, s); 2.53–2.39 (4H, m); 1.75–1.65 (4H, m). Anal. Calcd for $C_{20}H_{22}N_4O$: C, 71.83; H, 6.63; N, 16.75. Found: C, 71.68; H, 6.67; N, 16.61.

4.3.13. 6-(4-Dimethylaminomethylphenyl)-pyrrolo[2,3-*b*]pyridin-1-carboxylic acid bis-(4-methoxybenzyl)amide (15)

From compound **14**. Heated for 3 h at 100 °C. Flash column chromatography (CH_2Cl_2 :MeOH 95:5). Yield 57%; sticky solid; 1H NMR ($CDCl_3$) δ 8.05–7.92 (3H, m); 7.67 (1H, d, $J = 8.1$ Hz); 7.61 (1H, d, $J = 3.7$ Hz); 7.56–7.47 (2H, m); 7.41 (1H, m); 7.30–7.10 (3H, m); 6.92–6.79 (4H, m); 6.62 (1H, d, $J = 3.7$ Hz); 4.61 (4H, s); 3.94 (2H, s); 3.81 (6H, s); 2.61 (6H, s). Anal. Calcd for $C_{33}H_{34}N_4O_3$: C, 74.13; H, 6.41; N, 10.48. Found: C, 74.28; H, 6.45; N, 10.59.

4.4. 6-Biphenyl-4-yl-1H-pyrrolo[2,3-*b*]pyridine (6f) ³²

A flask charged with 4-bromobiphenyl (100 mg, 0.43 mmol), bispinacolate diboron (100 mg, 0.47 mmol), $PdCl_2(dppf)CH_2Cl_2$ (9.4 mg, 0.01 mmol), KOAc (126 mg, 1.29 mmol) in dioxane (2.60 mL) was heated for 5 h at 100 °C under nitrogen. After cooling the solution to room temperature, compound **5** (169 mg, 0.86 mmol), $PdCl_2(dppf)CH_2Cl_2$ (9.4 mg, 0.013 mmol), 2 M Na_2CO_3 (0.54 mL, 1.07 mmol) were added and the mixture was stirred at 100 °C for 4 h. The solution was cooled to room temperature and

the product was extracted with ethyl acetate. The organic layer was washed with 0.25 M HCl, dried, filtered and evaporated. Purification by flash chromatography (hexane:ethyl acetate 85:15) gave **6f** (57%) as a white solid; mp 245 °C; ¹H NMR (DMSO-*d*₆) δ 11.72 (1H, br s); 8.19 (2H, d, *J* = 7.9 Hz); 8.02 (1H, d, *J* = 8.4 Hz); 7.84–7.60 (5H, m); 7.55–7.32 (4H, m); 6.46 (1H, m). Anal. Calcd for C₁₉H₁₄N₂: C, 84.42; H, 5.22; N, 10.36. Found: C, 84.66; H, 5.18; N, 10.48.

4.5. 2-(1*H*-Pyrrolo[2,3-*b*]pyridin-6-yl)-pyrrole-1-carboxylic acid tert-butyl ester (**6i**)³³

A nitrogen purged mixture of **5** (200 mg, 1.01 mmol), N-Boc-2-pyrroleboronic acid (321 mg, 1.52 mmol), K₂CO₃ (279 mg, 2.02 mmol) and Pd(Ph₃)₄ (58.4 mg, 0.05 mmol) in DME:H₂O 4:1 (5.5 mL) was stirred at 100 °C for 3 h in the dark. The mixture was diluted with CH₂Cl₂ and washed with aqueous NH₄Cl. The aqueous phase was re-extracted with CH₂Cl₂ and the combined organic extracts were dried over Na₂SO₄ and concentrated in vacuo. Purification by flash chromatography (hexane:diethyl ether 6:4) afforded **6i** (84%) as a light yellow solid; mp 136 °C; ¹H NMR (CDCl₃) δ 12.00 (1H, br s); 7.95 (1H, d, *J* = 8.1 Hz); 7.45 (1H, m); 7.27–7.16 (2H, m); 6.51–6.43 (2H, m); 6.33 (1H, m); 1.18 (9H, s). Anal. Calcd for C₁₆H₁₇N₃O₂: C, 67.83; H, 6.05; N, 14.83. Found: C, 67.99; H, 6.00; N, 14.97.

4.6. General procedure B²⁵

To a solution of 7-hydroxy-1*H*-pyrrolo[2,3-*b*]pyridinium 3-chlorobenzoate (5.15 mmol)³⁰ and dimethyl sulfate (5.67 mmol) in anhydrous MeCN (10 mL) were stirred overnight under N₂ at 55–60 °C. After cooling to room temperature, the amine (25.5 mmol) was added and the mixture was stirred overnight under N₂ at 55–60 °C. After cooling to room temperature, the suspension was concentrated under reduced pressure and the residue partitioned between CH₂Cl₂ (10 mL) and 10% aqueous Na₂CO₃ (2.5 mL). The aqueous phase was extracted with CH₂Cl₂ (3 × 5 mL) and the combined organic layers were washed with 10% aqueous Na₂CO₃ (3 mL), brine (3 mL), H₂O (3 mL) and dried over Na₂SO₄ and evaporated under reduced pressure. The crude was purified by flash column chromatography. Following this procedure compounds **6p–r** were prepared.

4.6.1. 6-Pyrrolidin-1-yl-1*H*-pyrrolo[2,3-*b*]pyridine (**6p**)

Heated for 12 h at 55–60 °C, then 8 h at 50–55 °C. Flash column chromatography (hexane:ethyl acetate 7:3). Yield 56%; white solid; mp 218 °C; ¹H NMR (DMSO-*d*₆) δ 10.98 (1H, br s); 7.63 (1H, d, *J* = 8.4 Hz); 6.91 (1H, m); 6.23 (1H, d, *J* = 8.4 Hz); 6.17 (1H, m); 3.35–3.28 (4H, m); 1.99–1.84 (4H, m). Anal. Calcd for C₁₁H₁₃N₃: C, 70.56; H, 7.00; N, 22.44. Found: C, 70.41; H, 7.04; N, 22.22.

4.6.2. 6-(4-Methyl-piperazin-1-yl)-1*H*-pyrrolo[2,3-*b*]pyridine (**6q**)

Heated for 12 h at 55–60 °C, then 12 h at 50–55 °C. Flash column chromatography (CH₂Cl₂:MeOH 92:8). Yield 29%; white solid; mp 197 °C; ¹H NMR (DMSO-*d*₆) δ 11.00 (1H, br s); 7.67 (1H, d, *J* = 8.6 Hz); 7.02 (1H, m); 6.60 (1H, d, *J* = 8.6 Hz); 6.19 (1H, m); 3.46–3.37 (4H, m); 2.42–2.35 (4H, m); 2.20 (3H, s). Anal. Calcd for C₁₂H₁₆N₄: C, 66.64; H, 7.46; N, 25.90. Found: C, 66.51; H, 7.42; N, 26.01.

4.6.3. 6-Piperidin-1-yl-1*H*-pyrrolo[2,3-*b*]pyridine (**6r**)

Heated for 12 h at 55–60 °C, then 8 h at 50–55 °C. Flash column chromatography (Hexane:ethyl acetate 8:2). Yield 35%; sticky solid; ¹H NMR (CDCl₃) δ 8.72 (1H, br s); 7.73 (1H, d, *J* = 8.5 Hz); 6.98 (1H, m); 6.60 (1H, d, *J* = 8.5 Hz); 6.33 (1H, m); 3.60–3.48 (4H, m); 1.75–1.60 (6H, m). Anal. Calcd for C₁₂H₁₅N₃: C, 71.61; H, 7.51; N, 20.88. Found: C, 71.87; H, 7.55; N, 20.66.

4.7. General procedure C

Compound **6** (2.5 mmol) was added to a solution of triphosgene (1 mmol) and DIPEA (5.5 mmol) in toluene (0.35 mL). The mixture was heated at 80 °C for 1.5–3 h, then it was cooled to room temperature and NH₃/CH₂Cl₂ (3 mL saturated solution) was added. After stirring overnight at room temperature, ethyl acetate was added and the organic phase was washed twice with 0.25 M HCl, twice with saturated NaHCO₃ solution, then dried and evaporated. The residue was purified by flash chromatography.

Following this procedure compounds **1b–f**, **1i**, **1p** were prepared.

4.7.1. 6-Phenyl-pyrrolo[2,3-*b*]pyridine-1-carboxylic acid amide (**1b**)

Heated 90 min at 80 °C. Flash chromatography (hexane:ethyl acetate 75:25). Yield 46%; white solid; mp 205 °C. ¹H NMR (CDCl₃) δ 9.86 (1H, br s); 8.01–7.91 (4H, m); 7.69 (1H, d, *J* = 8.2 Hz); 7.58–7.41 (3H, m); 6.61 (1H, d, *J* = 3.8 Hz); 5.63 (1H, br s). Anal. Calcd for C₁₄H₁₁N₃O: C, 70.87; H, 4.67; N, 17.71. Found: C, 70.64; H, 4.63; N, 17.91.

4.7.2. 6-(4-Methoxy-phenyl)-pyrrolo[2,3-*b*]pyridine-1-carboxylic acid amide (**1c**)

Heated 2 h at 80 °C. Flash chromatography (hexane: acetone 75:25). Yield 29%; white solid; mp 199 °C; ¹H NMR (CDCl₃) δ 9.88 (1H, br s); 8.02–7.88 (4H, m); 7.62 (1H, d, *J* = 8.4 Hz); 7.04 (2H, d, *J* = 8.6 Hz); 6.59 (1H, d, *J* = 4.4 Hz); 5.58 (1H, br s); 3.90 (3H, s). Anal. Calcd for C₁₅H₁₃N₃O₂: C, 67.40; H, 4.90; N, 15.72. Found: C, 67.61; H, 4.95; N, 15.66.

4.7.3. 6-(4-Dimethylamino-phenyl)-pyrrolo[2,3-*b*]pyridine-1-carboxylic acid amide (**1d**)

Stirred 2 h at room temperature. Flash chromatography (dichloromethane:acetone 99:1). Yield 46%; white solid; mp 222 °C; ¹H NMR (DMSO-*d*₆) δ 9.26 (1H, br s); 8.10 (1H, br s); 8.08 (1H, d, *J* = 8.2 Hz); 7.90 (2H, d, *J* = 9.1 Hz); 7.85 (1H, d, *J* = 4.1 Hz); 7.75 (1H, d, *J* = 8.2 Hz); 6.82 (2H, d, *J* = 9.1 Hz); 6.65 (1H, d, *J* = 4.1 Hz); 2.76 (6H, s). Anal. Calcd for C₁₆H₁₆N₄O: C, 68.55; H, 5.75; N, 19.99. Found: C, 68.70; H, 5.98; N, 20.08.

4.7.4. 6-(4-Fluoro-phenyl)-pyrrolo[2,3-*b*]pyridine-1-carboxylic acid amide (**1e**)

Heated 2.5 h at 80 °C. Flash chromatography (hexane:ethyl acetate 80:20). Yield 85%; white solid; mp 174 °C; ¹H NMR (CDCl₃) δ 9.75 (1H, br s); 8.01 (1H, d, *J* = 8.1 Hz); 7.99–7.88 (3H, m); 7.61 (1H, d, *J* = 8.1 Hz); 7.19 (2H, t, *J* = 8.8 Hz); 6.59 (1H, d, *J* = 4.4 Hz); 5.62 (1H, br s). Anal. Calcd for C₁₄H₁₀FN₃O: C, 65.88; H, 3.95; N, 16.46. Found: C, 65.65; H, 3.99; N, 16.67.

4.7.5. 6-Biphenyl-4-yl-pyrrolo[2,3-*b*]pyridine-1-carboxylic acid amide (**1f**)

Heated 3 h at 80 °C. Flash chromatography (hexane:ethyl acetate 80:20), then crystallization from diethyl ether. Yield 76%; white solid; mp 235 °C; ¹H NMR (DMSO-*d*₆) δ 9.16 (1H, br s); 8.26–8.12 (4H, m), 7.98–7.91 (2H, m), 7.83 (2H, d, *J* = 8.2 Hz); 7.75 (2H, d, *J* = 7.4 Hz); 7.54–7.45 (2H, m); 7.39 (1H, t, *J* = 7.0 Hz); 6.73 (1H, d, *J* = 4.0 Hz). Anal. Calcd for C₂₀H₁₅N₃O: C, 76.66; H, 4.82; N, 13.41. Found: 76.49; H, 4.86; N, 13.61.

4.7.6. 6-(1*H*-Pyrrol-2-yl)-pyrrolo[2,3-*b*]pyridine-1-carboxylic acid amide (**1i**)

Heated 1 h at 80 °C. Flash chromatography (dichloromethane:acetone 197:3) gave 2-(1-carbamoyl-1*H*-pyrrolo[2,3-*b*]pyridin-6-yl)-pyrrole-1-carboxylic acid tert-butyl ester. Yield 74%; white solid; mp 186 °C. ¹H NMR (CDCl₃) δ 9.58 (1H, br s);

7.99–7.90 (2H, m); 7.38 (1H, m); 7.34 (1H, d, $J = 8.1$ Hz); 6.56 (1H, m); 6.43 (1H, m); 6.27 (1H, m); 5.42 (1H, br s); 1.32 (9H, s).

Removal of Boc protecting group was accomplished by refluxing a solution of the above compound (40 mg, 0.123 mmol) in MeOH (1.5 mL)/10.2 N HCl (0.016 mL) for 5 h. Methanol was evaporated and the residual slurry was added with CH_2Cl_2 . The organic phase was washed with 10% Na_2CO_3 , dried, filtered and evaporated. Purification by flash chromatography (CH_2Cl_2 : acetone 95:5) gave **1i** (59%); ^1H NMR ($\text{DMSO}-d_6$) δ 11.75 (1H, br s); 8.92 (1H, br s); 7.98 (1H, d, $J = 8.2$ Hz); 7.91 (1H, br s); 7.81 (1H, d, $J = 3.8$ Hz); 7.60 (1H, d, $J = 8.2$ Hz); 6.92 (1H, m); 6.79 (1H, d, $J = 3.9$ Hz); 6.59 (1H, m); 6.15 (1H, d, $J = 4.0$ Hz). Anal. Calcd for $\text{C}_{12}\text{H}_{10}\text{N}_4\text{O}$: C, 63.71; H, 4.46; N, 24.77. Found: C, 63.88; H, 4.50; N, 24.61.

4.7.7. 6-Pyrrolidin-1-yl-pyrrolo[2,3-*b*]pyridine-1-carboxylic acid amide (**1p**)

Heated for 1 h at 80 °C in toluene. Flash column chromatography (hexane:ethyl acetate 75:25). Yield 80%; white solid; mp 198 °C; ^1H NMR ($\text{DMSO}-d_6$) δ 9.11 (1H, br s); 7.83 (1H, m); 7.77 (1H, d, $J = 8.9$ Hz); 7.45 (1H, d, $J = 4.0$ Hz); 6.43 (1H, br s); 6.41 (1H, d, $J = 4.0$ Hz); 3.42–3.32 (4H, m); 2.01–1.90 (4H, m). Anal. Calcd for $\text{C}_{12}\text{H}_{14}\text{N}_4\text{O}$: C, 62.59; H, 6.13; N, 24.33. Found: C, 62.39; H, 6.18; N, 24.45.

4.8. General procedure D

A solution of **6** (1 mmol) and 4-nitrophenylchloroformate (1.6 mmol) in toluene (18 mL, for **7g**, **h**, **k**, **q**, **r**, **8**) or CH_2Cl_2 (18 mL for **7j**) containing NaOH (3 mmol) and a catalytic amount of Bu_4NBr (0.05 mmol) was heated (40–100 °C) for 2–7 h under a stream of nitrogen. Ethyl acetate was added and the organic phase was washed with water, dried over Na_2SO_4 and filtered. Following this procedure compounds **7g**, **h**, **j**, **k**, **q**, **r**, **8** were prepared.

4.8.1. 6-(2-Fluoro-phenyl)-pyrrolo[2,3-*b*]pyridine-1-carboxylic acid 4-nitro-phenyl ester (**7g**)

Heated for 2 h at 60 °C. Used for the next step without further purification.

4.8.2. 6-[3-(4-Cyclopropanecarbonyl-piperazine-1-carbonyl)-4-fluoro-phenyl]-pyrrolo[2,3-*b*]pyridine-1-carboxylic acid 4-nitro-phenyl ester (**7h**)

Heated for 3 h at 100 °C. Used for the next step without further purification.

4.8.3. 6-(4-Morpholin-4-ylmethyl-phenyl)-pyrrolo[2,3-*b*]pyridine-1-carboxylic acid 4-nitro-phenyl ester (**7k**)

Heated for 7 h at 40 °C. Used for the next step without further purification.

4.8.4. 6-[4-(Piperidine-1-carbonyl)-phenyl]-pyrrolo[2,3-*b*]pyridine-1-carboxylic acid 4-nitro-phenyl ester (**7j**)

Stirred for 4 h at room temperature. Used for the next step without further purification.

4.8.5. 6-(4-Methyl-piperazin-1-yl)-pyrrolo[2,3-*b*]pyridine-1-carboxylic acid 4-nitro-phenyl ester (**7q**)

Heated for 2 h at 100 °C in toluene. Flash column chromatography (CH_2Cl_2 :MeOH 95:5). Yield 51%; sticky solid; ^1H NMR (CDCl_3) δ 8.36 (2H, d, $J = 9.1$ Hz); 7.74 (1H, d, $J = 8.7$ Hz); 7.56–7.48 (3H, m); 6.69 (1H, d, $J = 8.7$ Hz); 6.54 (1H, d, $J = 3.7$ Hz); 3.92–3.64 (4H, m); 2.87–2.65 (4H, m); 2.45 (3H, s). Anal. Calcd for $\text{C}_{19}\text{H}_{19}\text{N}_5\text{O}_4$: C, 59.84; H, 5.02; N, 18.36. Found: C, 59.66; H, 5.05; N, 18.18.

4.8.6. 6-Piperidin-1-yl-pyrrolo[2,3-*b*]pyridine-1-carboxylic acid 4-nitro-phenyl ester (**7r**)

Heated for 3.5 h at 75 °C. Used for the next step without further purification.

4.8.7. 6-Bromo-pyrrolo[2,3-*b*]pyridine-1-carboxylic acid 4-nitro-phenyl ester (**8**)

From compound **5**. Stirred for 1 h at room temperature. Used without further purification.

4.9. General procedure E

To a solution of **7** (1 mmol) in dry DMF (3.6 mL) $(\text{NH}_4)_2\text{CO}_3$ (1.6 mmol) was added and the mixture was heated at 40–60 °C for 0.5–2.5 h. After addition of water (10 mL) the mixture was extracted with EtOAc (3×10 mL). The combined organic layers were washed with brine (50 mL), dried over Na_2SO_4 , filtered and evaporated. Following this procedure compounds **1g–h**, **j**, **k**, **q**, **r**, **9** were prepared.

4.9.1. 6-(2-Fluoro-phenyl)-pyrrolo[2,3-*b*]pyridine-1-carboxylic acid amide (**1g**)

Heated 1 h at 60 °C. Flash column chromatography (hexane:ethyl acetate 4:3) then crystallization from diethyl ether. Yield 58%; yellow solid; mp 186 °C; ^1H NMR (CDCl_3) δ 9.73 (1H, br s); 8.05–7.98 (2H, m); 7.84 (1H, t, $J = 7.6$ Hz); 7.69 (1H, d, $J = 8.2$ Hz); 7.42–7.16 (3H, m); 6.61 (1H, d, $J = 4.0$ Hz); 5.52 (1H, br s). Anal. Calcd for $\text{C}_{14}\text{H}_{10}\text{FN}_3\text{O}$: C, 65.88; H, 3.95; N, 16.46. Found: C, 65.67; H, 3.92; N, 16.66.

4.9.2. 6-[3-(4-Cyclopropanecarbonyl-piperazine-1-carbonyl)-4-fluoro-phenyl]-pyrrolo[2,3-*b*]pyridine-1-carboxylic acid amide (**1h**)

Heated 2.5 h at 60 °C. Flash column chromatography (hexane:acetone 6:4) then crystallization from $\text{CH}_2\text{Cl}_2/\text{Et}_2\text{O}$. Yield 23%; white solid; mp 184 °C; ^1H NMR ($\text{DMSO}-d_6$) δ 9.60 (1H, br s); 8.08–7.93 (4H, m); 7.62 (1H, d, $J = 8.1$ Hz); 7.26 (1H, m); 6.60 (1H, d, $J = 4.0$ Hz); 5.74 (1H, br s); 3.99–3.57 (6H, m); 3.53–3.30 (2H, m); 1.92 (1H, m); 1.06–0.98 (2H, m); 0.91–0.67 (2H, m). Anal. Calcd for $\text{C}_{23}\text{H}_{22}\text{FN}_5\text{O}_3$: C, 63.44; H, 5.09; N, 16.08. Found: C, 63.21; H, 5.13; N, 15.95.

4.9.3. 6-[4-(Piperidine-1-carbonyl)-phenyl]-pyrrolo[2,3-*b*]pyridine-1-carboxylic acid amide (**1j**)

Heated 0.5 h at 40 °C. Flash column chromatography (CH_2Cl_2 :MeOH 197:3). Yield 72%; white solid; mp 179 °C; ^1H NMR (CDCl_3) δ 9.77 (1H, br s); 8.09–7.93 (4H, m); 7.68 (1H, d, $J = 8.1$ Hz); 7.52 (2H, d, $J = 7.3$ Hz); 6.60 (1H, d, $J = 3.2$ Hz); 5.64 (1H, br s); 3.78–3.31 (4H, m); 1.94–1.48 (6H, m). Anal. Calcd for $\text{C}_{20}\text{H}_{20}\text{N}_4\text{O}_2$: C, 68.95; H, 5.79; N, 16.08. Found: C, 69.08; H, 5.72; N, 16.23.

4.9.4. 6-(4-Morpholin-4-ylmethyl-phenyl)-pyrrolo[2,3-*b*]pyridine-1-carboxylic acid amide (**1k**)

Heated 3 h at 45 °C. Flash column chromatography (CH_2Cl_2 :MeOH 96:4). Yield 50%; mp 162 °C; ^1H NMR (CDCl_3) δ 9.82 (1H, br s); 8.05–7.89 (4H, m); 7.66 (1H, d, $J = 7.9$ Hz); 7.60–7.35 (2H, m); 6.59 (1H, d, $J = 4.0$ Hz); 5.60 (1H, br s); 3.90–3.45 (6H, m); 2.69–2.39 (4H, m). Anal. Calcd for $\text{C}_{19}\text{H}_{20}\text{N}_4\text{O}_2$: C, 67.84; H, 5.99; N, 16.66. Found: C, 67.64; H, 5.93; N, 16.83.

4.9.5. 6-(4-Methyl-piperazin-1-yl)-pyrrolo[2,3-*b*]pyridine-1-carboxylic acid amide (**1q**)

Heated for 1 h at 45 °C. Flash column chromatography (CH_2Cl_2 :MeOH 9:1). Yield 78%; white solid; mp 142 °C; ^1H NMR (CDCl_3) δ 9.34 (1H, br s); 7.75 (1H, d, $J = 8.8$ Hz); 7.68 (1H, d, $J = 3.8$ Hz); 6.66 (1H, d, $J = 8.8$ Hz); 6.40 (1H, d, $J = 3.8$ Hz); 5.53 (1H, br s);

3.75–3.42 (4H, m); 2.91–2.60 (4H, m); 2.45 (3H, s). Anal. Calcd for $C_{13}H_{17}N_5O$: C, 60.21; H, 6.61; N, 27.01. Found: C, 60.08; H, 6.67; N, 26.88.

4.9.6. 6-Piperidin-1-yl-pyrrolo[2,3-*b*]pyridine-1-carboxylic acid amide (1r)

Heated for 0.5 h at 40 °C. Flash column chromatography (CH_2Cl_2 :MeOH 98:12). Yield 62%; white solid; mp 148 °C; 1H NMR ($CDCl_3$) δ 9.55 (1H, br s); 7.71 (1H, d, J = 8.7 Hz), 7.64 (1H, d, J = 3.8 Hz); 6.66 (1H, d, J = 8.7 Hz); 6.39 (1H, d, J = 3.8 Hz); 5.58 (1H, br s); 3.54–3.50 (4H, m); 1.80–1.60 (6H, m). Anal. Calcd for $C_{13}H_{16}N_4O$: C, 63.91; H, 6.60; N, 22.93. Found: C, 64.08; H, 6.55; N, 22.73.

4.9.7. 6-Bromo-pyrrolo[2,3-*b*]pyridine-1-carboxylic acid amide (9)

From compound **8**. Heated 1 h at 50 °C. Quantitative yield; sticky solid; 1H NMR ($CDCl_3$) δ 9.02 (1H, br s); 7.95 (1H, d, J = 3.9 Hz); 7.81 (1H, d, J = 8.1 Hz); 7.37 (1H, d, J = 8.1 Hz); 6.59 (1H, d, J = 3.9 Hz); 5.59 (1H, br s). Anal. Calcd for $C_8H_6BrN_3O$: C, 40.03; H, 2.52; N, 17.50. Found: C, 40.23; H, 2.55; N, 17.68.

4.10. 6-(4-Piperidin-1-ylmethyl-phenyl)-pyrrolo[2,3-*b*]pyridine-1-carboxylic acid amide (1l)³⁴

(a) A solution of lithium hexamethyldisilazane in THF (0.28 mL, 1.0 M, 0.28 mmol) was added to a solution of **6l** (75 mg, 0.26 mmol) in THF (3 mL) at –78 °C. The reaction was stirred at –78 °C for 40 min, whereupon 4-nitrophenylchloroformate (104 mg, 0.51 mmol) was added portionwise over 5 min., then the cooling bath was removed and stirring continued for 2 h. Saturated aq. NH_4Cl (2 mL) was added and the mixture was extracted with CH_2Cl_2 (3×20 mL). The combined organic layers were dried over Na_2SO_4 and concentrated under reduced pressure. The residue was purified by flash chromatography (CH_2Cl_2 : MeOH 95:5) to obtain **1l** (17%) as a white solid; mp 177–178 °C; 1H NMR ($CDCl_3$) δ 9.82 (1H, br s); 8.03–7.94 (2H, m); 7.90 (2H, d, J = 7.8 Hz); 7.64 (1H, d, J = 8.2 Hz); 7.47 (2H, d, J = 7.8 Hz); 6.58 (1H, d, J = 4.0 Hz); 5.59 (1H, br s); 3.59 (2H, s); 2.58–2.38 (4H, m); 1.75–1.54 (4H, m); 1.50–1.39 (2H, m). Anal. Calcd for $C_{20}H_{22}N_4O$: C, 71.83; H, 6.63; N, 16.75. Found: C, 71.99; H, 6.603; N, 16.55.

(b) A solution of **19** (1.900 g, 4.2 mmol) in 145 mL of TFA was refluxed for 34 h. TFA was evaporated under vacuum and the residue was dissolved in ethyl acetate. The organic phase was washed three times with a cold saturated solution of $NaHCO_3$, then it was dried, filtered and evaporated. The crude (2.07 g) was first crystallized from $AcOEt/Et_2O$ and then purified by flash chromatography (CH_2Cl_2 : MeOH 95: 5) to obtain the title compound as a white solid (64%); mp 178 °C. 1H NMR ($CDCl_3$) δ 9.82 (1H, br s); 8.03–7.94 (2H, m); 7.90 (2H, d, J = 7.8 Hz); 7.64 (1H, d, J = 8.2 Hz); 7.47 (2H, d, J = 7.8 Hz); 6.58 (1H, d, J = 4.0 Hz); 5.59 (1H, br s); 3.59 (2H, s); 2.58–2.38 (4H, m); 1.75–1.54 (4H, m); 1.50–1.39 (2H, m). Anal. Calcd for $C_{20}H_{22}N_4O$: C, 71.83; H, 6.63; N, 16.75. Found: C, 71.98; H, 6.72; N, 16.84.

4.11. 2-(6-Bromo-pyrrolo[2,3-*b*]pyridin-1-yl)-acetamide (10)

Compound **5** (200 mg, 1.01 mmol) dissolved in dry DMF (0.61 mL) was added dropwise to a suspension of NaH (60% in mineral oil) in dry DMF (0.81 mL) and the mixture was stirred for 30 min at room temperature. Iodoacetamide (187 mg, 1.01 mmol) dissolved in DMF (1.01 mL) was added dropwise and the reaction was stirred for 3 h at room temperature. Iced water was added (20 mL) and the mixture was extracted with ethyl acetate (3×20 mL). The combined organic phases were dried, filtered and the solvent was evaporated to give 229 mg (89%) of the desired

compound as a white solid; mp 223 °C; 1H NMR ($DMSO-d_6$) δ 7.94 (1H, d, J = 8.8 Hz); 7.64 (1H, br s); 7.51 (1H, d, J = 3.5 Hz); 7.26 (1H, d, J = 8.8 Hz); 7.25 (1H, br s); 6.51 (1H, d, J = 3.5 Hz); 4.85 (2H, s). Anal. Calcd for $C_9H_8BrN_3O$: C, 42.54; H, 3.17; N, 16.54. Found: C, 42.69; H, 3.12; N, 16.36.

4.12. 6-Bromo-pyrrolo[2,3-*b*]pyridine-1-carboxylic acid bis-(4-methoxybenzyl)amide (14)

A solution of **8** (138 mg, 0.38 mmol) and bis-(4-methoxybenzyl)amine (**13**)²⁴ (158 mg, 0.61 mmol) in anhydrous DMF (1.5 mL) was heated at 60 °C for 6 h. After addition of ethyl acetate, the solution was washed with water and brine, then it was dried over Na_2SO_4 , filtered and evaporated. Purification by flash column chromatography (hexane: ethyl acetate 8:2) afforded 109 mg (91%) of the title compound as a sticky solid; 1H NMR ($CDCl_3$) δ 7.78 (1H, d, J = 8.2 Hz); 7.50 (1H, d, J = 3.8 Hz); 7.35 (1H, d, J = 8.2 Hz); 7.32–7.15 (4H, m); 6.95–6.80 (4H, m); 6.58 (1H, d, J = 3.8 Hz); 4.55 (4H, s); 3.80 (6H, s). Anal. Calcd for $C_{24}H_{22}BrN_3O_3$: C, 60.01; H, 4.62; N, 8.75. Found: C, 60.21; H, 4.66; N, 8.55.

4.13. 6-(4-Dimethylaminomethyl-phenyl)-pyrrolo[2,3-*b*]pyridine-1-carboxylic acid amide (1o)

Compound **15** (27 mg, 0.05 mmol) was refluxed in TFA (2 mL) for 9.5 h. TFA was then removed under vacuum and the residue was added with CH_2Cl_2 , washed with a saturated solution of $NaHCO_3$, dried, filtered and evaporated. Purification by PLC (CH_2Cl_2 : MeOH 17:3) afforded 11 mg (78%) of the title compound as a white solid; mp 199 °C; 1H NMR ($CDCl_3$) δ 9.81 (1H, br s); 8.04–7.88 (4H, m); 7.66 (1H, d, J = 8.1 Hz); 7.50 (2H, d, J = 7.9 Hz); 6.59 (1H, d, J = 3.7 Hz); 5.72 (1H, br s); 3.65 (2H, s); 2.40 (6H, s). Anal. Calcd for $C_{17}H_{18}N_4O$: C, 69.37; H, 6.16; N, 19.03. Found: C, 69.08; H, 6.21; N, 18.83.

4.14. (4-Methoxybenzyl)carbamic acid isopropenyl ester (17)

To a solution of NaOH (348 mg, 8.7 mmol) in water (4 mL) *p*-methoxybenzylamine (0.76 mL, 5.8 mmol) in ethyl acetate (9.7 mL) was added dropwise, while keeping the temperature below 5 °C. After cooling to 0 °C, isopropenyl chloroformate (1.00 g, 8.2 mmol) was added and the reaction mixture was stirred at room temperature for 3 h. The layers were separated. The organic layer was dried over Na_2SO_4 , filtered and evaporated. The crude product (1.4 g) was used for the next step without further purification.

4.15. 6-Bromo-pyrrolo[2,3-*b*]pyridine-1-carboxylic acid 4-methoxybenzylamide (18)

To a solution of 6-bromo-7-azaindole (0.500 g, 2.5 mmol) in anhydrous THF (12 mL) under nitrogen, NaH (60% in mineral oil, 0.130 g, 3.25 mmol) was added and the resulting mixture was stirred at room temperature for 2 h. A solution of **17** (0.978 g, 4.42 mmol) in anhydrous THF (8 mL) was then added and the mixture was stirred at room temperature for 20 h. The solvent was evaporated and water was added. The aqueous phase was extracted with ethyl acetate (3×30 mL). The collected organic layers were dried, filtered and evaporated to give 1.19 g of a crude that was purified by column chromatography (Hexane: ethyl acetate 9:1). The title compound was obtained as a white solid (79%); mp 97 °C; 1H NMR ($CDCl_3$) δ 9.47 (1H, br s); 7.98 (1H, d, J = 3.5 Hz); 7.79 (1H, d, J = 7.8 Hz); 7.45–7.31 (3H, m); 6.91 (2H, d, J = 8.4 Hz); 6.52 (1H, d, J = 3.5 Hz); 4.60 (2H, m); 3.80 (3H, s). Anal. Calcd for $C_{16}H_{14}BrN_3O_2$: C, 53.35; H, 3.92; N, 11.67. Found: C, 53.56; H, 3.96; N, 11.48.

4.16. 6-(4-Piperidin-1-ylmethyl-phenyl)-pyrrolo[2,3-b]pyridine-1-carboxylic acid-4-methoxy-benzylamide (19)

To a suspension of **18** (1.700 g, 4.7 mmol) in 3.5:1 DME/H₂O (18 mL) under nitrogen, 1-[4-(4,4,5,5-tetramethyl-[1,3,2]dioxaborolan-2-yl)-benzyl]-piperidine (95%, 1.67 g, 5.2 mmol), NaHCO₃ (1.18 g, 14 mmol), PdCl₂(dppf)CH₂Cl₂ (0.139 g, 0.19 mmol) were added and the resulting mixture was refluxed for 45 min. in the dark. After evaporation of the solvent the residue was added with water/ethyl acetate. The phases were separated. The organic layer was dried, filtered and evaporated to obtain 3.00 g of crude. Purification by flash chromatography (CH₂Cl₂: MeOH 98:2) gave 1.9 g (89%) of the title compound; mp 93 °C; ¹H NMR (CDCl₃) δ 10.26 (1H, t, *J* = 4.4 Hz); 8.01 (1H, d, *J* = 4.0 Hz); 7.97 (1H, d, *J* = 8.2 Hz); 7.70–7.60 (3H, m); 7.42 (2H, d, *J* = 8.5 Hz); 7.30 (2H, d; *J* = 8.2 Hz); 6.94 (2H, d, *J* = 8.5 Hz); 6.54 (1H, d, *J* = 3.96 Hz); 4.67 (2H, d, *J* = 4.4 Hz); 3.86 (3H, s); 3.52 (2H, s); 2.53–2.31 (4H, m); 1.72–1.51 (6H, m). Anal. Calcd for C₂₈H₃₀N₄O₂: C, 73.98; H, 6.65; N, 12.33. Found: C, 73.77; H, 6.61; N, 12.52.

4.17. Biological assays

The purity of all tested compounds was assessed by HPLC and was \geq 95%.

4.17.1. PARP-1 enzyme assay

Enzymatic assay was carried out by means of a highly sensitive fluorescent assay (HT-F Homogeneous Inhibition Assay; Trevigen) according to the manufacturer's instructions. Briefly, damaged DNA was mixed with increasing amounts of NAD⁺ (0–100 nM) and then incubated, for 30 min, with recombinant human PARP-1 enzyme (expressed as GST fusion protein in *Escherichia coli* cells), in the presence or absence of serial dilutions (dose-response curve) of test compounds. Reactions were terminated by the addition of a stop solution containing resazurin and, finally, after 30 min of incubation, the resazurin-dependent fluorescence was quantified by a multiplate reader (Victor; Perkin Elmer). A NAD standard curve was generated within each assay. IC₅₀ values for inhibitors were calculated by means of the ALLFIT software.

4.17.2. Cell lines

The pancreatic adenocarcinoma Capan 1, the breast cancer HCC1937 and the endometrial carcinoma HeLa cell lines were obtained from American Type Culture Collection. The ovarian sensitive and multidrug resistant, respectively A2780 and A2780/Dx were kindly provided by Istituto Nazionale dei Tumori di Milano. The breast carcinoma MX-1 cell lines were from CLS (Cells Line Service). All tumor cell lines were of human origin and were grown in RPMI-1640, containing L-glutamine supplemented with 10% heat-inactivated fetal calf serum (FCS, Life Technologies), except than the HCC1937 cell line which was cultured in IMDM medium plus 20% foetal calf serum.

4.17.3. Cell sensitivity studies

Cell sensitivity to drugs was evaluated by growth inhibition assays based on cell counting (HCC1937 and Capan 1) or SRB assays (A2780 and A2780/Dx). HCC1937 and Capan 1 cells were seeded in duplicates into 6-well plates and exposed to drug 24 h later. The studied compounds were dissolved in dimethylsulfoxide (DMSO) and then added to culture medium. DMSO concentration in medium never exceeded 0.25%. After 72 h of drug incubation, cells were harvested for counting with a cell counter. A2780 and A2780/Dx cells were grown in a volume of 200 μ L at approximately 10% confluency in 96-well multititer plates and were allowed to recover for an additional 24 h. Tumor cells were treated with either varying concentrations of drugs or solvent for 72 h. The fraction of cells

surviving after compound treatment was determined using the SRB assay. IC₅₀ is defined as the drug concentration producing 50% decrease of cell growth. At least three independent experiments were performed. The resistance index as the ratio between IC₅₀ of resistant and sensitive cells was evaluated.

4.17.4. PARylation assay

HeLa cells were seeded into 96-well Viewplate black microplates, in culture medium. The plates were incubated for 4/6 h, at 37 °C, under 5% CO₂ atmosphere, then the test compounds were added with serial dilutions, over six points. The plates were incubated for 3 h at 37 °C in 5% CO₂, then DNA damage was provoked by addition of 5 μ L of H₂O₂ solution in H₂O (final concentration 200–500 μ M). As a negative control, cells untreated with H₂O₂ were used. The plates were kept at 37 °C for 5 min, and then cells were fixed by addition of ice-cold MeOH (100 μ L/well) and kept at –20 °C for 20 min. Following fixation, cells were repeatedly washed with PBS and then protein PARylation was detected using the primary PAR mAb (Alexis ALX-804-220, 1:2000) and the secondary anti-mouse Alexa Fluor 488 antibody (Molecular probes A11029, 1:3000). Nuclei were stained with the specific nuclear dye Draq5 (Alexis, 5 μ M). After 3 h incubation at room temperature in the dark, cells were extensively washed with PBS and, finally, fluorescence was read on the high content imaging system 'Operetta' (Perkin Elmer). Fluorescence signals related to the residual amount of PAR polymer on nuclear proteins were measured at the optimal wavelengths (excitation/emission), and identification of the nuclei within cells was performed by tracking Draq5. The percent of PAR-positive cells was calculated at last by measuring the ratio between the numbers of PAR-positive nuclei over the total number of Draq5-labeled nuclei. Finally, for the active test compounds, the IC₅₀ values were determined on the basis of the residual enzyme activity in the presence of increasing concentration of test compounds.

4.17.5. In vivo tumor model

Female mice, SCID beige of 22–24 g from Charles River were used. Mice were housed inside cages of makrolon (33.2 \times 15 \times 13 cm) (4 mice/cage) with stainless steel cover-feed and sterilized and dust-free bedding cobs. Nude mice were maintained in cages with paper filter covers; food and bedding were sterilized and water was acidified. Animals were housed under a light-dark cycle, keeping temperature and humidity constant. Parameters of the animal rooms were assessed as follows: 22 \pm 2 °C temperature, 55 \pm 10% relative humidity, about 15–20 filtered air changes/hour and 12 h circadian cycle of artificial light (7 a.m., 7 p.m.). At request, the environmental conditions were monitored and the data were retained in Animal Housing Archives. Experimental protocols were approved by the Ethic Committee for Animal Experimentation according to the United Kingdom Coordinating Committee on Cancer Research Guidelines. MX-1 cell lines were inoculated subcutaneously (5 \times 10⁶/200 μ L/mouse in RGF matrigel 50:50). Starting 7 days after tumor injection, mice (8 mice/group) were treated with in the following experimental groups: Vehicle (10% DMSO+10% of 2-hydroxypropylbetacyclodextrin in PBS), ST7710 100 mg/10 mL/kg ip (q2d/wx2w), AZD-2281 (ST7437) 167 mg/10 mL/kg ip (q2d/wx2w). Body weight recordings were carried out through the study and mortality was noted. To evaluate the antitumor activity of the drugs, tumor diameters were measured biweekly with a Vernier caliper. The formula TV (mm³) = [length (mm) \times width (mm)²]/2 was used, where the width and the length are the shortest and the longest diameters of each tumor, respectively. When tumors reached a weight of about 0.5 g, mice were sacrificed by cervical dislocation. Toxicity of the molecule was determined as: body weight loss percent (% BWL max) = 100 – (mean BW_{day x}/mean BW_{day 1} \times 100), where

BW_x is the mean BW at the day of maximal loss during the treatment and BW₁ is the mean BW on the 1st day of treatment. Lethal toxicity was also evaluated. Efficacy of the molecule was evaluated as tumor volume inhibition (TVI%) according to the equation: % TVI = 100 – [(mean tumor weight of treated mice/mean tumor weight of control group) × 100]. For statistical comparison, TVs of experimental groups were compared by Mann–Whitney's test.

4.17.6. Molecular modeling

The models were built based on the crystal structure of PARP catalytic domain in complex with novel inhibitors (PDB code 4HHY).³⁵ After the separation of the coordinates of ligands, cofactors, water molecules and enzyme, polar hydrogens were added with the GROMACS package³⁶ using the GROMOS 53a6 force field.³⁷ The structures of the ligands were refined using a systematic conformer, search followed by geometry optimization of the lowest energy structure with NWChem (RMS gradient 0.0010).³⁸ Molecular docking experiments were performed with Autodock 4.0, which uses an empirical scoring function based on the free energy of binding.^{39,40} The ligands and the PARP catalytic domain were further processed using the Autodock Tool Kit (ADT).⁴¹ Gasteiger–Marsili charges⁴² were assigned and solvation parameters were added to the final docked structure using Addsol utility. Structures with less than 1.0 Å root-mean-square deviation (rmsd) were clustered together and representative model of each cluster was selected based on the most favourable free energy of binding. Visual inspection was carried out to select the final structure. In the current study, we used the combined quantum mechanical molecular mechanics (QM/MM) approach as implemented in NWChem.³⁸ The combined quantum mechanical molecular mechanics (QM/MM) approach provides a simple and effective tool to study localized molecular transformations in large scale systems such as those encountered in solution chemistry or enzyme catalysis. In this method an accurate but computationally intensive quantum mechanical (QM) description is only used for the regions where electronic structure transformations are occurring (e.g., bond making and breaking). The rest of the system, whose chemical identity remains essentially the same, is treated at the approximate classical molecular mechanics (MM) level. The QM/MM module in NWChem is built as a top level interface between the classical MD module and various QM modules, managing initialization, data transfer, and various high level operations. For the QM/MM calculations, the PARP–ligand systems resulting from the docking study were first partitioned into a QM subsystem and an MM subsystem. The reaction system used a smaller QM subsystem consisting of the ligand and residues within 4.5 Å, whereas the rest of the system (the MM subsystem) was treated using a modified AMBER force field. The boundary problem between the QM and MM subsystems was treated using the pseudo-bond approach. With this QM/MM system, an iterative optimization procedure was applied to the QM/MM system, using 3-21G* QM/MM calculations, leading to an optimized structure for the reactants. The convergence criterion used was set to obtain an energy gradient of <10^{−4}, using the twin-range cutoff method for nonbonded interactions, with a long-range cutoff of 14 Å and a short-range cutoff of 8 Å.

References and notes

- Wahlberg, E.; Karlberg, T.; Kouznetsova, E.; Markova, N.; Macchiarulo, A.; Thorsell, A. G.; Pol, E.; Frostell, A.; Ekblad, T.; Öncü, D.; Kull, B.; Robertson, G. M.; Pellicciari, R.; Schüller, H.; Weigelt, J. *Nat. Biotechnol.* **2012**, *30*, 283.
- Javle, M.; Curtin, N. J. *Br. J. Cancer* **2011**, *105*, 1114.
- De Vos, M.; Schreiber, V.; Dantzer, F. *Biochem. Pharmacol.* **2012**, *84*, 137.
- (a) Powell, C.; Mikropoulos, C.; Kaye, S. B.; Nutting, C. M.; Bhide, S. A.; Newbold, K.; Harrington, K. J. *Cancer Treat. Rev.* **2010**, *36*, 566; (b) <http://clinicaltrials.gov/ct2/results?term=parp&Search=Search>.
- Farmer, H.; McCabe, N.; Lord, C. J.; Tutt, A. N.; Johnson, D. A.; Richardson, T. B.; Santarosa, M.; Dillon, K. J.; Hickson, I.; Knights, C.; Martin, N. M.; Jackson, S. P.; Smith, G. C.; Ashworth, A. *Nature* **2005**, *434*, 917.
- Bryant, H. E.; Schultz, N.; Thomas, H. D.; Parker, K. M.; Flower, D.; Lopez, E.; Kyle, S.; Meuth, M.; Curtin, N. J.; Helleday, T. *Nature* **2005**, *434*, 913.
- Maxwell, K. N.; Domchek, S. M. *Nat. Rev. Clin. Oncol.* **2012**, *9*, 520.
- Helleday, T. *Mol. Oncol.* **2011**, *5*, 387.
- (a) Welsby, I.; Hutin, D.; Leo, O. *Biochem. Pharmacol.* **2012**, *84*, 11; (b) Swindall, A. F.; Stanley, J. A.; Yang, E. S. *Cancers* **2013**, *5*, 943.
- Ma, Y.; Chen, H.; He, X.; Nie, H.; Hong, Y.; Sheng, C.; Wang, Q.; Xia, W.; Ying, W. *Curr. Drug Targets* **2012**, *2*, 222.
- Ferraris, D. V. *J. Med. Chem.* **2010**, *53*, 4561.
- Papeo, G.; Casale, E.; Montagnoli, A.; Cirila, A. *Exp. Opin. Ther. Pat.* **2013**, *23*, 503.
- Tinoco, G.; Warsch, S.; Glück, S.; Avancha, K.; Montero, A. J. *J. Cancer* **2013**, *4*, 117.
- (a) Curtin, N. J. *Drug Discovery Today* **2012**, *9*, 51; (b) Curtin, N. J.; Szabo, C. *Mol. Aspects Med.* **2013**, *34*, 1217.
- Costantino, G.; Macchiarulo, A.; Camaioni, E.; Pellicciari, R. *J. Med. Chem.* **2001**, *44*, 3786.
- Bellocci, D.; Macchiarulo, A.; Costantino, G.; Pellicciari, R. *Bioorg. Med. Chem.* **2005**, *13*, 1151.
- Zeng, H.; Zhang, H.; Jang, F.; Zhao, L.; Zhang, J. *Chem. Biol. Drug Des.* **2011**, *78*, 333.
- Fatima, S.; Bathini, R.; Sivan, S. K.; Manga, V. J. *Recept. Signal Transduction* **2012**, *32*, 214.
- Penning, T. D.; Zhu, G. D.; Gandhi, V. B.; Gong, J.; Liu, X.; Shi, Y.; Klinghofer, V.; Johnson, E. F.; Donawho, C. K.; Frost, D. J.; Bontcheva-Diaz, V.; Bouska, J. J.; Osterling, D. J.; Olson, A. M.; Marsh, K. C.; Luo, Y.; Giranda, V. L. *J. Med. Chem.* **2009**, *52*, 514.
- Karlberg, T.; Hammarstrom, M.; Schutz, P.; Svensson, L.; Schuler, H. *Biochemistry* **2010**, *49*, 1056.
- Minakata, S.; Komatsu, M.; Ohshiro, Y. *Synthesis* **1992**, 661.
- Ahaidar, A.; Fernandez, D.; Danelón, G.; Cuevas, C.; Manzanera, I.; Albericio, F.; Joule, J. A.; Alvarez, M. J. *Org. Chem.* **2003**, *68*, 10020.
- Jacquemard, U.; Bénéteau, V.; Lefoix, M.; Routier, S.; Mèrou, J.; Coudert, G. *Tetrahedron* **2004**, *60*, 10039.
- Anastasi, C.; Hantz, O.; De Clercq, E.; Pannecouque, C.; Clayette, P.; Dereuddre-Bosquet, N.; Dormont, D.; Gondois-Rey, F.; Hirsch, I.; Kraus, J. J. *Med. Chem.* **2004**, *47*, 1183.
- Storz, T.; Bartberger, M. D.; Sukits, S.; Wilde, C.; Soukup, T. *Synthesis* **2008**, 201.
- Gallou, I.; Eriksson, M.; Zeng, X.; Senanayake, C.; Farina, V. J. *Org. Chem.* **2005**, *70*, 6960.
- Veber, D. F.; Johnson, S. R.; Cheng, H. Y.; Smith, B. R.; Ward, K. W.; Kopple, K. D. *J. Med. Chem.* **2002**, *45*, 2615.
- Scarpelli, R.; Boueres, J. K.; Cerretani, M.; Ferrigno, F.; Ontoria, M.; Rowley, M.; Schults-Fademrecht, C.; Toniatti, C.; Jones, P. *Bioorg. Med. Chem. Lett.* **2010**, *20*, 488.
- Jones, P.; Altamura, S.; Boueres, J.; Ferrigno, F.; Fonsi, M.; Giomini, M. C.; Lamartina, S.; Monteagudo, E.; Ontoria, J. M.; Orsale, M. V.; Palumbi, M. C.; Pesci, S.; Roscilli, G.; Scarpelli, R.; Schults-Fademrecht, C.; Toniatti, C.; Rowley, M. J. *Med. Chem.* **2009**, *52*, 7170.
- Schneller, S. W.; Luo, J. J. *Org. Chem.* **1980**, *45*, 4045.
- (a) Dallavalle, S.; Cincinelli, R.; Nannei, R.; Merlini, L.; Morini, G.; Penco, S.; Pisano, C.; Vesci, L.; Barbarino, M.; Zucco, V.; De Cesare, M.; Zunino, F. *E. J. Med. Chem.* **2009**, *44*, 1900; (b) Cincinelli, R.; Dallavalle, S.; Nannei, R.; Carella, S.; De Zani, D.; Merlini, L.; Penco, S.; Garattini, E.; Giannini, G.; Pisano, C.; Vesci, L.; Carminati, P.; Zucco, V.; Zanchi, C.; Zunino, F. *J. Med. Chem.* **2005**, *48*, 4931.
- Giroux, A.; Han, Y.; Prasit, P. *Tetrahedron Lett.* **1997**, *38*, 3841.
- Nauš, P.; Pohl, R.; Votruba, I.; Džubák, P.; Hajdúch, M.; Ameral, R.; Birkuš, G.; Wang, T.; Ray, A. S.; Mackman, R.; Cihlar, T.; Hocke, M. *J. Med. Chem.* **2010**, *53*, 460.
- Petterson, M.; Knueppel, D.; Martin, S. F. *Org. Lett.* **2007**, *9*, 4623.
- Ye, N.; Chen, C. H.; Chen, T.; Song, Z.; He, J. X.; Huan, X. J.; Song, S. S.; Liu, Q.; Chen, Y.; Ding, J.; Xu, Y.; Miao, Z. H.; Zhang, A. *J. Med. Chem.* **2013**, *56*, 2885.
- Lindahl, E.; Hess, B.; van der Spoel, D. *J. Mol. Model.* **2001**, *7*, 306.
- Oostenbrink, C.; Soares, T. A.; van der Vegt, N. F. A.; van Gunsteren, W. F. *Eur. Biophys. J. Biophys. Lett.* **2005**, *34*, 273.
- Valiev, M.; Bylaska, E. J.; Govind, N.; Kowalski, K.; Straatsma, T. P.; van Dam, H. J. J.; Wang, D.; Nieplocha, J.; Apra, E.; Windus, T. L.; de Jong, W. A. *Comput. Phys. Commun.* **2010**, *181*, 1477.
- Morris, G. M.; Goodsell, D. S.; Halliday, R. S.; Huey, R.; Hart, W. E.; Belew, R. K.; Olson, A. J. *J. Comput. Chem.* **1998**, *19*, 1639.
- Huey, R.; Morris, G. M.; Olson, A. J.; Goodsell, D. S. *J. Comput. Chem.* **2007**, *28*, 1145.
- Sanner, M. F. *J. Mol. Graph. Model.* **1999**, *17*, 57.
- Gasteiger, J.; Marsili, M. *Tetrahedron* **1980**, *36*, 3219.